

Mass transport of impurities in a moderately dense granular gas

Vicente Garzó* and Francisco Vega Reyes†

Departamento de Física, Universidad de Extremadura, E-06071 Badajoz, Spain

(Dated: August 9, 2021)

Transport coefficients associated with the mass flux of impurities immersed in a moderately dense granular gas of hard disks or spheres described by the inelastic Enskog equation are obtained by means of the Chapman-Enskog expansion. The transport coefficients are determined as the solutions of a set of coupled linear integral equations recently derived for polydisperse granular mixtures [V. Garzó, J. W. Dufty and C. M. Hrenya, *Phys. Rev. E* **76**, 031304 (2007)]. With the objective of obtaining theoretical expressions for the transport coefficients that are sufficiently accurate for highly inelastic collisions, we solve the above integral equations by using the second Sonine approximation. As a complementary route, we numerically solve by means of the direct simulation Monte Carlo method (DSMC) the inelastic Enskog equation to get the kinetic diffusion coefficient D_0 for two and three dimensions. We have observed in all our simulations that the disagreement, for arbitrarily large inelasticity, in the values of both solutions (DSMC and second Sonine approximation) is less than 4%. Moreover, we show that the second Sonine approximation to D_0 yields a dramatic improvement (up to 50%) over the first Sonine approximation for impurity particles lighter than the surrounding gas and in the range of large inelasticity. The results reported in this paper are of direct application in important problems in granular flows, such as segregation driven by gravity and a thermal gradient. We analyze here the segregation criteria that result from our theoretical expressions of the transport coefficients.

I. INTRODUCTION

The theoretical basis for a hydrodynamic description of ordinary (elastic) gases is well established at low density using the Boltzmann kinetic equation. However, for moderately dense gases there is no accurate and practical generalization of the Boltzmann equation except for the idealized hard sphere fluid. For this intermolecular potential, the Enskog kinetic equation takes into account the dominant positional corrections to the Boltzmann equation due to excluded volume effects but, like the Boltzmann equation, neglects velocity correlations (molecular chaos assumption) among particles which are about to collide [1]. The Enskog equation is the only available theory at present for making explicit calculations of the transport properties of moderately dense gases and in any case the molecular chaos assumption is expected to fail only in much denser systems (solid volume fractions typically are larger than 0.4) [2]. The extension to mixtures requires a revision of the original Enskog theory for thermodynamic consistency (revised Enskog theory, or RET) [3], and its application to hydrodynamics and Navier-Stokes (NS) transport coefficients was carried out more than twenty years ago [4].

Early attempts [5, 6, 7, 8] to extend the study of López de Haro, Cohen and Kincaid [4] to *inelastic* hard sphere mixtures were restricted to nearly elastic systems. In this case, the effect of inelasticity in the collisions is taken into account only by the presence of a sink term in the energy balance equation and, as a consequence, the expressions of the NS transport coefficients are the same as those obtained for elastic systems. Moreover, those early works also assume energy equipartition and so the partial temperatures for each species are equal to the granular temperature. However, as the dissipation increases, different species of a granular mixture have different partial temperatures T_i and consequently, the energy equipartition is seriously broken down ($T_i \neq T$) [9, 10, 11]. The failure of energy equipartition in granular fluids has also been confirmed by computer simulations [12] and observed in real experiments [13] of agitated mixtures. Results in the literature show that the deviation from equipartition depends on the size and mass ratios of the particles of each species and the coefficients of restitution of the system.

A more general extension of the RET to inelastic collisions has been recently carried out by Garzó, Dufty and Hrenya [14, 15]. This theory covers some of the aspects not taken into account in previous works [5, 6, 7, 8] and extends previous results derived for monodisperse dense systems [16, 17] and dilute binary mixtures [18]. Specifically, (i) it goes beyond the weak dissipation limit so that it is expected to be applicable to a wide range of coefficients of restitution, (ii) it takes into account the non-equipartition of granular energy, and (iii) it has been formulated for multicomponent systems without limits on the number of components. Therefore, this theory [14] subsumes all previous analysis for both ordinary and granular gases, which are recovered in the appropriate limits [4, 16, 17, 18].

* Electronic address: vicenteg@unex.es; URL: <http://www.unex.es/eweb/fisteor/vicente/>

† Electronic address: fvega@unex.es

Nevertheless, as in the elastic case [4], although the results are exact in the first order of spatial gradients, the explicit form of the NS transport coefficients requires to solve a set of linear integral equations. The standard method to get the kinetic and collisional contributions to transport coefficients and cooling rate consists of approximating the solutions to these integral equations by Maxwellians (at different temperatures) times truncated Sonine polynomial expansions. For simplicity, usually only the lowest Sonine polynomial (first Sonine approximation) is retained [15], and the results obtained from this approximation compare very well with Monte Carlo simulations of the Enskog equation in the case of the shear viscosity coefficient of a mixture heated by an external thermostat [19]. However, exceptions to this good agreement are extreme mass or size ratios and strong dissipation, although these discrepancies could be mitigated in part if one considers higher-order terms in the Sonine polynomial expansion, as previous studies in the dilute limit indicate [20]. In fact, recent works for monodisperse gases have shown that higher order terms in Sonine polynomial expansions become increasingly important in the range of moderate and strong inelasticities [22, 23], and for this reason it has been of interest to calculate transport coefficients with more refined Sonine approaches [24, 25]. However, the above works have been mainly focused with low density granular gases and many of the problems of practical interest in granular gases lie in the range of moderate densities. For this reason, it is important to determine the degree of accuracy of at least the first Sonine approximation compared to the second Sonine approximation for dense granular gases. Therefore, by testing an eventual gain of accuracy with higher order Sonine approximations, our results in the present work will contribute to the debate in the literature on the validity of a hydrodynamic description of granular gases [21]. In addition, the range of high inelasticities has growing interest in experimental works [26, 27]. Another motivation to improve the evaluation of the NS transport coefficients lies in the fact that the reference homogeneous cooling state (HCS) is known to suffer a clustering instability, with inter-cluster distance inversely proportional to inelasticity [28]. In this context, we believe that a more accurate description of the HCS in the range of mild and strong inelasticities may help to refine the understanding of this interesting instability.

Needless to say, the evaluation of the NS transport coefficients for a dense granular mixture beyond the first Sonine approximation is quite intricate, due mainly to the coupling among the different integral equations obeying the transport coefficients. We will thus make a first approach to the problem by considering the simple situation of a granular binary mixture where the concentration of one of the species (of mass m_0 and diameter σ_0) is very small (impurity or tracer limit). Moreover, the tracer limit has been of much interest in recent literature, for example in granular segregation problems [29, 30, 31, 32]. In the case of a tracer immersed in a dense granular gas, and as in a previous study for dilute gases [20], one can assume that (i) the state of the dense gas (excess component of mass m and diameter σ) is not affected by the presence of impurities or tracer particles and, (ii) one can also neglect collisions among tracer particles in their corresponding kinetic equation. As a consequence, the velocity distribution function f of the gas verifies a closed Enskog equation while the velocity distribution function f_0 of the tracer particles obeys the linear Enskog-Lorentz equation, which greatly simplifies the development of Chapman-Enskog theory.

Under the above conditions, since the pressure tensor and heat flux of the mixture (gas plus impurities) is the same as that for the gas [16, 17], the mass transport of impurities \mathbf{j}_0 is the relevant flux of the tracer problem. To first order in the spatial gradients, three transport coefficients are involved in the constitutive equation for \mathbf{j}_0 : the kinetic diffusion coefficient D_0 , the mutual diffusion coefficient D and the thermal diffusion coefficient D^T . Thus, the mass flux \mathbf{j}_0 has the form [14]

$$\mathbf{j}_0 = -\frac{m_0^2}{\rho} D_0 \nabla n_0 - \frac{mm_0}{\rho} D \nabla n - \frac{\rho}{T} D^T \nabla T, \quad (1)$$

where $\rho = mn$ is the total mass density, n_0 is the number density of the impurities, n is the number density of the gas particles, and T is the granular temperature. Therefore, the main goal of this paper is to determine D_0 , D and D^T up to the second Sonine approximation in terms of the coefficients of restitution for the impurity-gas (α_0) and gas-gas (α) collisions, the parameters of the system (masses and sizes) and the solid volume fraction ϕ occupied by the gas. The calculations are rather intricate and we have taken advantage of some previous calculations performed in Ref. [15] for multicomponent systems. In particular, a previous expression for the coefficient D_0 obtained in the second Sonine approximation for a dilute gas ($\phi = 0$) is recovered [20]. Analogously to the previous analysis of the shear viscosity coefficient [19], kinetic theory predictions for the diffusion coefficient D_0 are compared with numerical solutions of the Enskog equation by using the well-known direct simulation Monte Carlo (DSMC) method [33]. In the simulations, the diffusion coefficient is computed from the mean-square displacement of impurities immersed in a dense granular gas undergoing the homogeneous cooling state [20]. Although the problem is time-dependent, a transformation to a convenient set of dimensionless time and space variables [34] allows one to get a stationary diffusion equation where the coefficient D_0 can be measured in the hydrodynamic regime (times large compared with the characteristic mean free time).

Finally, once the explicit expression of the transport coefficients associated with the mass flux are at hand, a segregation criterion based on thermal diffusion is derived. This criterion shows the transition between the well-known Brazil-nut effect (BNE) and the reverse Brazil-nut effect (RBNE) by varying the different parameters of the

system. This study complements a previous analysis recently carried out by one of the authors [32] for a driven (heated) dense gas. As expected, our results show that the form of the phase-diagrams for the BNE/RBNE transition depends sensitively on the value of gravity relative to the thermal gradient and so it is possible to switch between both states for given values of the parameters of the system.

The plan of the paper is as follows. In Sec. II we describe the problem we are interested in and offer a short summary of the set of inelastic Enskog equations for the gas and the impurities. Section III deals with the application of the Chapman-Enskog method [35] to solve the Enskog-Lorentz equation and get the set of coupled linear integral equations verifying the transport coefficients D_0 , D and D^T . Then, these integral equations are approximately solved up to the second Sonine approximation. Some technical details of the calculations are given in Appendices A and B. In Sec. IV we illustrate the dependence of the transport coefficients on the parameters of the system and compare the theoretical results for the coefficient D_0 obtained in the first and second Sonine approximation with those obtained by means of Monte Carlo simulations of the Enskog-Lorentz equation for disks ($d = 2$) and spheres ($d = 3$). Segregation by thermal diffusion is studied in Sec. V and the paper is closed in Sec. VI with a brief discussion on the results derived.

II. DESCRIPTION OF THE PROBLEM

Let us consider a binary mixture of inelastic particles with collision rules according to the smooth hard sphere model. Our system is described by the revised Enskog kinetic equation [36, 37] and, as a starting point, we consider in this work the special case where the concentration of one of the components (the tracer or intruder) is very small compared to that of the other (solvent or excess) component. In this limit, the state of the granular gas (the solvent) is not affected by the presence of the tracer particles and also the mutual interactions among the tracer particles can be neglected as compared with their interactions with the particles of the solvent. At a kinetic theory level, this implies that the velocity distribution function of the solvent (f) and of the tracer particles (f_0) obey respectively the closed (nonlinear) Enskog equation and the (linear) Enskog-Lorentz equation. This is formally equivalent to study an impurity or intruder in a dense granular gas, and this will be the terminology used here. Since in the tracer limit the pressure tensor and the heat flux of dense binary mixtures are the same as those of the pure excess component (in the absence of the tracer), here we will be interested in the evaluation of the transport coefficients defining the mass flux of the intruder.

Let us start by offering a short review on some basic aspects of the set of inelastic Enskog equations for the gas and the intruder. The granular dense gas is composed by smooth inelastic hard disks ($d = 2$) or spheres ($d = 3$) of mass m and diameter σ . The inelasticity of collisions among all pairs is accounted for by a *constant* coefficient of normal restitution α ($0 \leq \alpha \leq 1$) that only affects the translational degrees of freedom of grains. The granular gas is in the presence of a gravitational field $\mathbf{g} = -g\hat{\mathbf{e}}_z$, where g is a positive constant and $\hat{\mathbf{e}}_z$ is the unit vector in the positive direction of the z axis. At moderate densities, we assume that the time evolution of the one-particle velocity distribution function of the gas $f(\mathbf{r}, \mathbf{v}, t)$ is given by the Enskog equation [36, 37]

$$\left(\partial_t + \mathbf{v} \cdot \nabla + \mathbf{g} \cdot \frac{\partial}{\partial \mathbf{v}} \right) f(\mathbf{r}, \mathbf{v}, t) = J[\mathbf{v}|f(t), f(t)], \quad (2)$$

where the Enskog collision operator $J[\mathbf{v}|f, f]$ is

$$\begin{aligned} J[\mathbf{r}_1, \mathbf{v}_1 | f(t), f(t)] \equiv & \sigma^{d-1} \int d\mathbf{v}_2 \int d\hat{\boldsymbol{\sigma}} \Theta(\hat{\boldsymbol{\sigma}} \cdot \mathbf{g}_{12}) (\hat{\boldsymbol{\sigma}} \cdot \mathbf{g}_{12}) \\ & \times [\alpha^{-2} \chi(\mathbf{r}_1, \mathbf{r}_1 - \boldsymbol{\sigma}) f(\mathbf{r}_1, \mathbf{v}_1''; t) f(\mathbf{r}_1 - \boldsymbol{\sigma}, \mathbf{v}_2''; t) \\ & - \chi(\mathbf{r}_1, \mathbf{r}_1 + \boldsymbol{\sigma}) f(\mathbf{r}_1, \mathbf{v}_1; t) f(\mathbf{r}_1 + \boldsymbol{\sigma}, \mathbf{v}_2; t)]. \end{aligned} \quad (3)$$

Here, σ is the hard sphere diameter, $\hat{\boldsymbol{\sigma}}$ is a unit vector along their line of centers, Θ is the Heaviside step function, and $\mathbf{g}_{12} = \mathbf{v}_1 - \mathbf{v}_2$ is the relative velocity. The primes on the velocities denote the initial values $\{\mathbf{v}_1'', \mathbf{v}_2''\}$ that lead to $\{\mathbf{v}_1, \mathbf{v}_2\}$ following a binary collision in the hard sphere model:

$$\mathbf{v}_1'' = \mathbf{v}_1 - \frac{1}{2} (1 + \alpha^{-1}) (\hat{\boldsymbol{\sigma}} \cdot \mathbf{g}_{12}) \hat{\boldsymbol{\sigma}}, \quad \mathbf{v}_2'' = \mathbf{v}_2 + \frac{1}{2} (1 + \alpha^{-1}) (\hat{\boldsymbol{\sigma}} \cdot \mathbf{g}_{12}) \hat{\boldsymbol{\sigma}}. \quad (4)$$

The quantity $\chi(\mathbf{r}_1, \mathbf{r}_1 + \boldsymbol{\sigma} | n(t))$ is the pair correlation function at contact as a functional of the nonequilibrium density field $n(\mathbf{r}, t)$, where

$$n(\mathbf{r}, t) = \int d\mathbf{v} f(\mathbf{r}, \mathbf{v}, t). \quad (5)$$

In addition, the flow velocity and the *granular* temperature are defined respectively as

$$\mathbf{u}(\mathbf{r}, t) = \frac{1}{n(\mathbf{r}, t)} \int d\mathbf{v} \mathbf{v} f(\mathbf{r}, \mathbf{v}, t), \quad (6)$$

$$T(\mathbf{r}, t) = \frac{m}{dn(\mathbf{r}, t)} \int d\mathbf{v} V^2 f(\mathbf{r}, \mathbf{v}, t), \quad (7)$$

where $\mathbf{V}(\mathbf{r}, t) \equiv \mathbf{v} - \mathbf{u}(\mathbf{r}, t)$ is the peculiar velocity. The macroscopic balance equations for number density n , momentum density $m\mathbf{u}$, and energy density $\frac{d}{2}nT$ follow directly from Eq. (2) by multiplying with 1, $m\mathbf{v}$, and $\frac{1}{2}mv^2$ and integrating over \mathbf{v} :

$$D_t n + n \nabla \cdot \mathbf{u} = 0, \quad (8)$$

$$D_t \mathbf{u} + (mn)^{-1} \nabla \cdot \mathbf{P} = \mathbf{g}, \quad (9)$$

$$D_t T + \frac{2}{dn} (\nabla \cdot \mathbf{q} + P_{ij} \nabla_j u_i) = -\zeta T, \quad (10)$$

where $D_t = \partial_t + \mathbf{u} \cdot \nabla$ is the material time derivative. The microscopic expressions for the pressure tensor \mathbf{P} , the heat flux \mathbf{q} , and the cooling rate ζ in terms of the velocity distribution function f can be found in Refs. [16] and [17]. Their explicit forms will be omitted here for brevity.

Let us suppose now that an impurity or intruder of mass m_0 and diameter σ_0 is added to the gas. As said before, the presence of the intruder does not have any effect on the state of the gas, so that its velocity distribution function is still determined by the Enskog equation (2). In addition, the macroscopic flow velocity and temperature for the mixture composed by the dense gas plus the intruder are the same as those for the gas, namely they are given by Eqs. (6) and (7), respectively. Under these conditions, the velocity distribution function $f_0(\mathbf{r}, \mathbf{v}, t)$ of the intruder satisfies the linear Enskog-Lorentz equation

$$\left(\frac{\partial}{\partial t} + \mathbf{v} \cdot \nabla + \mathbf{g} \cdot \frac{\partial}{\partial \mathbf{v}} \right) f_0(\mathbf{r}, \mathbf{v}, t) = J_0[\mathbf{v}|f_0(t), f(t)], \quad (11)$$

where the collision operator $J_0[\mathbf{v}|f_0(t), f(t)]$ is now

$$\begin{aligned} J_0[\mathbf{r}_1, \mathbf{v}_1|f_0(t), f(t)] &= \bar{\sigma}^{d-1} \int d\mathbf{v}_2 \int d\hat{\boldsymbol{\sigma}} \Theta(\hat{\boldsymbol{\sigma}} \cdot \mathbf{g}_{12}) (\hat{\boldsymbol{\sigma}} \cdot \mathbf{g}_{12}) \\ &\quad \times [\alpha_0^{-2} \chi_0(\mathbf{r}_1, \mathbf{r}_1 - \bar{\boldsymbol{\sigma}}) f_0(\mathbf{r}_1, \mathbf{v}_1''; t) f(\mathbf{r}_1 - \bar{\boldsymbol{\sigma}}, \mathbf{v}_2''; t) \\ &\quad - \chi_0(\mathbf{r}_1, \mathbf{r}_1 + \bar{\boldsymbol{\sigma}}) f_0(\mathbf{r}_1, \mathbf{v}_1; t) f(\mathbf{r}_1 + \bar{\boldsymbol{\sigma}}, \mathbf{v}_2; t)]. \end{aligned} \quad (12)$$

Here, $\bar{\boldsymbol{\sigma}} = \bar{\sigma} \hat{\boldsymbol{\sigma}}$, $\bar{\sigma} = (\sigma_0 + \sigma)/2$, α_0 ($0 \leq \alpha_0 \leq 1$) is the coefficient of restitution for intruder-gas collisions, and χ_0 is the pair correlation function for intruder-gas pairs at contact. The precollisional velocities are given by

$$\begin{aligned} \mathbf{v}_1'' &= \mathbf{v}_1 - \frac{m}{m_0 + m} (1 + \alpha_0^{-1}) (\hat{\boldsymbol{\sigma}} \cdot \mathbf{g}_{12}) \hat{\boldsymbol{\sigma}}, \\ \mathbf{v}_2'' &= \mathbf{v}_2 + \frac{m_0}{m_0 + m} (1 + \alpha_0^{-1}) (\hat{\boldsymbol{\sigma}} \cdot \mathbf{g}_{12}) \hat{\boldsymbol{\sigma}}. \end{aligned} \quad (13)$$

As shown in Ref. [11], the operator $J_0[\mathbf{v}|f_0, f]$ is the same as that of an *elastic* impurity ($\alpha_0 = 1$) with an effective mass

$$m_0^* = m_0 + \frac{1 - \alpha_0}{1 + \alpha_0} (m_0 + m). \quad (14)$$

The number density for the intruder is

$$n_0(\mathbf{r}, t) = \int d\mathbf{v} f_0(\mathbf{r}, \mathbf{v}, t). \quad (15)$$

The intruder may freely lose or gain momentum and energy in its interactions with the particles of the gas and, therefore, these are not invariants of the collision operator $J_0[\mathbf{v}|f_0, f]$. Only the number density n_0 is conserved, whose continuity equation is directly obtained from Eq. (11)

$$D_t n_0 + n_0 \nabla \cdot \mathbf{u} + \frac{\nabla \cdot \mathbf{j}_0}{m_0} = 0, \quad (16)$$

where \mathbf{j}_0 is the mass flux for the intruder, relative to the local flow \mathbf{u} ,

$$\mathbf{j}_0 = m_0 \int d\mathbf{v} \mathbf{V} f_0(\mathbf{r}, \mathbf{v}, t). \quad (17)$$

At a kinetic level, an interesting quantity is the local temperature of the intruder, defined as

$$T_0(\mathbf{r}, t) = \frac{m_0}{dn_0(\mathbf{r}, t)} \int d\mathbf{v} V^2 f_0(\mathbf{r}, \mathbf{v}, t). \quad (18)$$

This quantity measures the mean kinetic energy of the intruder. As confirmed by computer simulations [12], experiments [13] and kinetic theory calculations [9], the global temperature T and the temperature of the intruder T_0 are in general different, so that the granular energy per particle is not equally distributed between both components of the system.

III. MASS TRANSPORT OF IMPURITIES

In order to compute the mass flux \mathbf{j}_0 of impurities to first order in the spatial gradients, we solve the Enskog-Lorentz equation by means of the Chapman-Enskog (CE) expansion [35]. This method, nowadays extensively used and tested in a variety of problems in the field of rapid granular flows [38], assumes the existence of a *normal* solution in which all the space and time dependence of f_0 occurs through the hydrodynamic fields n_0 , n , \mathbf{u} and T . The CE procedure generates the normal solution explicitly by means of an expansion in the gradients of the fields:

$$f_0 = f_0^{(0)} + \epsilon f_0^{(1)} + \dots, \quad (19)$$

where ϵ is a formal parameter measuring the nonuniformity of the system. The application of the CE method to the Enskog equation for polydisperse granular mixtures has been carried out very recently [14, 15]. Using those results, we consider here the tracer limit ($x_0 \equiv n_0/n \rightarrow 0$) for the linear integral equations defining the transport coefficients associated with the mass flux. The first-order contribution $\mathbf{j}_0^{(1)}$ to the mass flux is given by Eq. (1), where the kinetic diffusion coefficient D_0 , the mutual diffusion coefficient D , and the thermal diffusion coefficient D^T are defined as

$$D^T = -\frac{m_0}{\rho d} \int d\mathbf{v} \mathbf{V} \cdot \mathcal{A}_0(\mathbf{V}), \quad (20)$$

$$D_0 = -\frac{\rho}{m_0 n_0 d} \int d\mathbf{v} \mathbf{V} \cdot \mathcal{B}_0(\mathbf{V}), \quad (21)$$

$$D = -\frac{1}{d} \int d\mathbf{v} \mathbf{V} \cdot \mathcal{C}_0(\mathbf{V}). \quad (22)$$

The quantities $\mathcal{A}_0(\mathbf{V})$, $\mathcal{B}_0(\mathbf{V})$, and $\mathcal{C}_0(\mathbf{V})$ are the solutions of the following set of coupled linear integral equations [14]:

$$\frac{1}{2} \zeta^{(0)} \frac{\partial}{\partial \mathbf{V}} \cdot (\mathbf{V} \mathcal{A}_0) - \frac{1}{2} \zeta^{(0)} \mathcal{A}_0 - J_0^{(0)}[\mathcal{A}_0, f^{(0)}] = \mathbf{A}_0 + J_0^{(0)}[f_0^{(0)}, \mathcal{A}], \quad (23)$$

$$\frac{1}{2} \zeta^{(0)} \frac{\partial}{\partial \mathbf{V}} \cdot (\mathbf{V} \mathcal{B}_0) - J_0^{(0)}[\mathcal{B}_0, f^{(0)}] = \mathbf{B}_0, \quad (24)$$

$$\frac{1}{2} \zeta^{(0)} \frac{\partial}{\partial \mathbf{V}} \cdot (\mathbf{V} \mathcal{C}_0) - n \frac{\partial \zeta^{(0)}}{\partial n} \mathcal{A}_0 - J_0^{(0)}[\mathcal{C}_0, f^{(0)}] = \mathbf{C}_0 + J_0^{(0)}[f_0^{(0)}, \mathcal{C}], \quad (25)$$

where $\zeta^{(0)}$ is the cooling rate to zeroth order (local homogeneous cooling state) and $J_0^{(0)}[X, Y]$ is the operator

$$J_0^{(0)}[\mathbf{v}_1|X, Y] = \chi_0^{(0)} \bar{\sigma}^{d-1} \int d\mathbf{v}_2 \int d\hat{\boldsymbol{\sigma}} \Theta(\hat{\boldsymbol{\sigma}} \cdot \mathbf{g}_{12})(\hat{\boldsymbol{\sigma}} \cdot \mathbf{g}_{12}) [\alpha_0^{-2} X(\mathbf{V}_1'') Y(\mathbf{V}_2'') - X(\mathbf{V}_1) Y(\mathbf{V}_2)], \quad (26)$$

where $\chi_0^{(0)}$ is the intruder-gas pair correlation function at zeroth order. The inhomogeneous terms of the integral equations (23)–(25) are defined by

$$A_{0,i}(\mathbf{V}) = \frac{1}{2} V_i \frac{\partial}{\partial \mathbf{V}} \cdot (\mathbf{V} f_0^{(0)}) - \frac{p}{\rho} \frac{\partial}{\partial V_i} f_0^{(0)} + \frac{1}{2} \mathcal{K}_{0,i} \left[\frac{\partial}{\partial \mathbf{V}} \cdot (\mathbf{V} f_0^{(0)}) \right], \quad (27)$$

$$\mathbf{B}_0(\mathbf{V}) = -\mathbf{V} f_0^{(0)}, \quad (28)$$

$$C_{0,i}(\mathbf{V}) = -m^{-1} \frac{\partial p}{\partial n} \frac{\partial}{\partial V_i} f_0^{(0)} - \frac{(1+\omega)^{-d}}{\chi_0^{(0)} T} \left(\frac{\partial \mu_0}{\partial \phi} \right)_{T, n_0} \mathcal{K}_{0,i} [f_0^{(0)}]. \quad (29)$$

In Eqs. (27)–(29), the pressure p is given by

$$p = nT \left[1 + 2^{d-2} \chi^{(0)} \phi (1 + \alpha) \right], \quad (30)$$

$\omega \equiv \sigma_0/\sigma$ is the size ratio and μ_0 is the chemical potential of the intruder. Furthermore,

$$\phi \equiv \frac{\pi^{d/2}}{2^{d-1} d \Gamma(d/2)} n \sigma^d \quad (31)$$

is the solid volume fraction and the operator $\mathcal{K}_{0,i}[X]$ is defined as

$$\mathcal{K}_{0,i}[X] = \bar{\sigma}^d \chi_0^{(0)} \int d\mathbf{v}_2 \int d\hat{\boldsymbol{\sigma}} \Theta(\hat{\boldsymbol{\sigma}} \cdot \mathbf{g}_{12})(\hat{\boldsymbol{\sigma}} \cdot \mathbf{g}_{12}) \hat{\sigma}_i \left[\alpha_0^{-2} f_0^{(0)}(\mathbf{V}_1'') X(\mathbf{V}_2'') + f_0^{(0)}(\mathbf{V}_1) X(\mathbf{V}_2) \right]. \quad (32)$$

Upon writing Eqs. (23)–(25), use has been made of the expression of the first-order distribution function $f^{(1)}$ of gas particles. Its form has been derived in Refs. [16, 17] and reads

$$f^{(1)} = \mathcal{A} \cdot \nabla T + \mathcal{C} \cdot \nabla n + \mathcal{D} : \nabla \mathbf{u} + E \nabla \cdot \mathbf{u}, \quad (33)$$

where the coefficients \mathcal{A} , \mathcal{C} , \mathcal{D} and E are functions of the peculiar velocity \mathbf{V} and the hydrodynamic fields. According to Eqs. (23)–(25), only the coefficients \mathcal{A} and \mathcal{C} are involved in the evaluation of the transport coefficients D_0 , D and D^T . The linear integral equations verifying \mathcal{A} and \mathcal{C} as well as their expressions up to the second Sonine approximation are given in Appendix A.

It is worthwhile to remark that the quantities \mathcal{A}_0 and \mathcal{C}_0 associated with the intruder are coupled with their corresponding counterparts \mathcal{A} and \mathcal{C} of the host gas through the integral equations (23) and (25), respectively. A direct consequence of this coupling is that the mass flux of the intruder (1) inherits gradient terms (∇n and ∇T) from those of the autonomous host equations. Moreover, the external field does not occur in the constitutive equation (1) for the mass flux. This is due to the particular form of the gravitational force.

IV. SECOND SONINE POLYNOMIAL APPROXIMATION

For practical purposes, the integral equations (23)–(25) can be solved by using a Sonine polynomial expansion. With the motivations explained in the Introduction, our goal here is to determine the diffusion coefficients D_0 and D and the thermal diffusion coefficient D^T up to the second Sonine approximation. In this case, the quantities \mathcal{A}_0 , \mathcal{B}_0 and \mathcal{C}_0 are approximated by

$$\mathcal{A}_0(\mathbf{V}) \rightarrow -f_{0,M}(\mathbf{V}) \left[\frac{\rho}{n_0 T_0} \mathbf{V} D^T + a_0 \mathbf{S}_0(\mathbf{V}) \right], \quad (34)$$

$$\mathcal{B}_0(\mathbf{V}) \rightarrow -f_{0,M}(\mathbf{V}) \left[\frac{m_0^2}{\rho T_0} \mathbf{V} D_0 + b_0 \mathbf{S}_0(\mathbf{V}) \right], \quad (35)$$

$$\mathcal{C}_0(\mathbf{V}) \rightarrow -f_{0,M}(\mathbf{V}) \left[\frac{m_0}{n_0 T_0} \mathbf{V} D + c_0 \mathbf{S}_0(\mathbf{V}) \right], \quad (36)$$

where

$$\mathbf{S}_0(\mathbf{V}) = \left(\frac{1}{2} m_0 V^2 - \frac{d+2}{2} T_0 \right) \mathbf{V}, \quad (37)$$

and $f_{0,M}(\mathbf{V})$ is a Maxwellian distribution at the temperature T_0 of the intruder, i.e.,

$$f_{0,M}(\mathbf{V}) = n_0 \left(\frac{m_0}{2\pi T_0} \right)^{d/2} \exp \left(-\frac{m_0 V^2}{2T_0} \right). \quad (38)$$

The coefficients a_0 , b_0 and c_0 are defined as

$$a_0 = -\frac{2}{d(d+2)} \frac{m_0}{n_0 T_0^3} \int d\mathbf{v} \mathbf{S}_0(\mathbf{V}) \cdot \mathcal{A}_0(\mathbf{V}), \quad (39)$$

$$b_0 = -\frac{2}{d(d+2)} \frac{m_0}{n_0 T_0^3} \int d\mathbf{v} \mathbf{S}_0(\mathbf{V}) \cdot \mathcal{B}_0(\mathbf{V}), \quad (40)$$

$$c_0 = -\frac{2}{d(d+2)} \frac{m_0}{n_0 T_0^3} \int d\mathbf{v} \mathbf{S}_0(\mathbf{V}) \cdot \mathcal{C}_0(\mathbf{V}). \quad (41)$$

The transport coefficients D_0 , D and D^T as well as the second Sonine coefficients a_0 , b_0 and c_0 are determined by substitution of Eqs. (34)–(36) into the integral equations (23)–(25), multiplication of these equations by $m_0 \mathbf{V}$ and by $\mathbf{S}_0(\mathbf{V})$, and integration over velocity. The details are carried out in Appendices B and C and only the final expressions will be presented here.

The second Sonine approximations $D_0[2]$, $D[2]$ and $D^T[2]$ can be written, respectively, as

$$D_0[2] = F(\alpha, \alpha_0, m_0/m, \sigma_0/\sigma, \phi) D_0[1], \quad (42)$$

$$D[2] = G(\alpha, \alpha_0, m_0/m, \sigma_0/\sigma, \phi) D[1], \quad (43)$$

$$D^T[2] = H(\alpha, \alpha_0, m_0/m, \sigma_0/\sigma, \phi) D^T[1], \quad (44)$$

where F , G and H are nonlinear functions of the mass and size ratios, the coefficients of restitution and the solid volume fraction. The explicit forms of F , G and H are given by Eqs. (B19), (B24) and (B17), respectively. In Eqs. (41)–(44), $D_0[1]$, $D[1]$ and $D^T[1]$ refer to the first Sonine approximations to D_0 , D and D^T , respectively. Their explicit expressions were already determined in Ref. [15] for arbitrary composition. In terms of the transport coefficients, the new calculations in the present work are the functions F , G , and H . In the tracer limit ($x_0 \rightarrow 0$), the expressions of $D_0[1]$, $D[1]$ and $D^T[1]$ reduce, respectively, to

$$D_0[1] = \frac{\rho T}{m_0^2 \nu} \frac{\gamma}{\nu_1^* - \frac{1}{2} \zeta^*}, \quad (45)$$

$$D[1] = \frac{n_0 T}{m_0 \nu} \frac{Y_1^*}{\nu_1^* - \frac{1}{2} \zeta^*}, \quad (46)$$

$$D^T[1] = \frac{n_0 T}{\rho \nu} \frac{X_1^*}{\nu_1^* - \zeta^*}. \quad (47)$$

Here, $\nu = n\sigma^{d-1} \sqrt{2T/m}$ is an effective collision frequency, $\gamma = T_0/T$ is the temperature ratio,

$$\zeta^* = \frac{\zeta^{(0)}}{\nu} = \frac{\sqrt{2}\pi^{(d-1)/2}}{d\Gamma(d/2)} \chi^{(0)} (1 - \alpha^2) \quad (48)$$

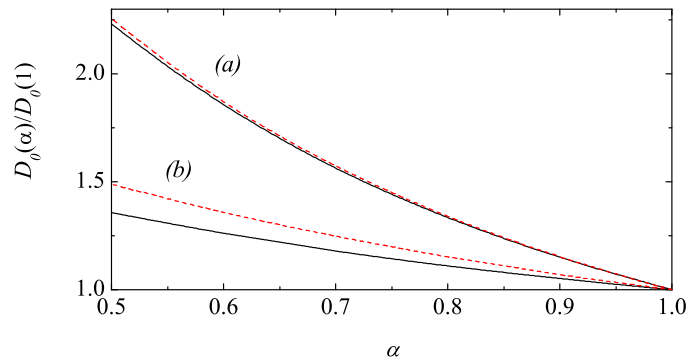


FIG. 1: (color online) Plot of the reduced kinetic diffusion coefficient $D_0(\alpha)/D_0(1)$ as a function of the (common) coefficient of restitution $\alpha = \alpha_0$ for the systems $(m_0/m = 4, \sigma_0/\sigma = 2)$ (a) and $(m_0/m = 0.5, \sigma_0/\sigma = 0.8)$ (b) in the case of a three-dimensional gas with $\phi = 0.1$. The solid lines correspond to the second Sonine approximation while the dashed lines refer to the first Sonine approximation. Here, $D_0(1)$ is the elastic value of the kinetic diffusion coefficient consistently obtained in each approximation.

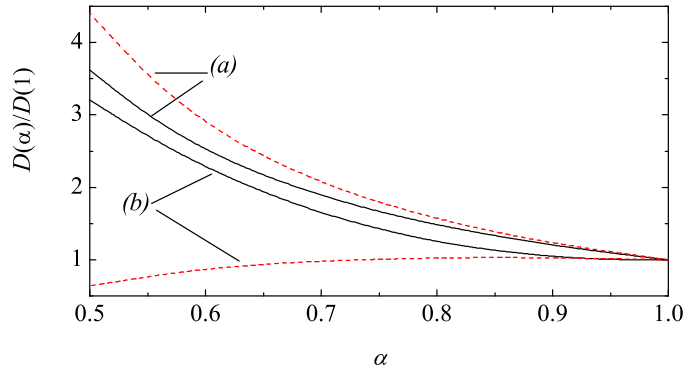


FIG. 2: (color online) Plot of the reduced mutual diffusion coefficient $D(\alpha)/D(1)$ as a function of the (common) coefficient of restitution $\alpha = \alpha_0$ for the systems $(m_0/m = 4, \sigma_0/\sigma = 2)$ (a) and $(m_0/m = 0.5, \sigma_0/\sigma = 0.8)$ (b) in the case of a three-dimensional gas with $\phi = 0.1$. The solid lines correspond to the second Sonine approximation while the dashed lines refer to the first Sonine approximation. Here, $D(1)$ is the elastic value of the kinetic diffusion coefficient consistently obtained in each approximation.

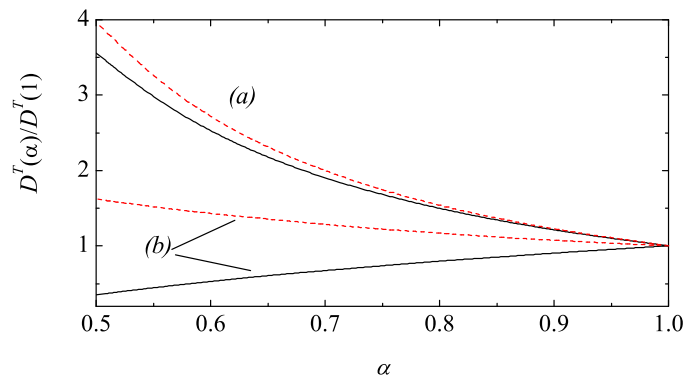


FIG. 3: (color online) Plot of the reduced thermal diffusion coefficient $D^T(\alpha)/D^T(1)$ as a function of the (common) coefficient of restitution $\alpha = \alpha_0$ for the systems $(m_0/m = 4, \sigma_0/\sigma = 2)$ (a) and $(m_0/m = 0.5, \sigma_0/\sigma = 0.8)$ (b) in the case of a three-dimensional gas with $\phi = 0.1$. The solid lines correspond to the second Sonine approximation while the dashed lines refer to the first Sonine approximation. Here, $D^T(1)$ is the elastic value of the thermal diffusion coefficient consistently obtained in each approximation.

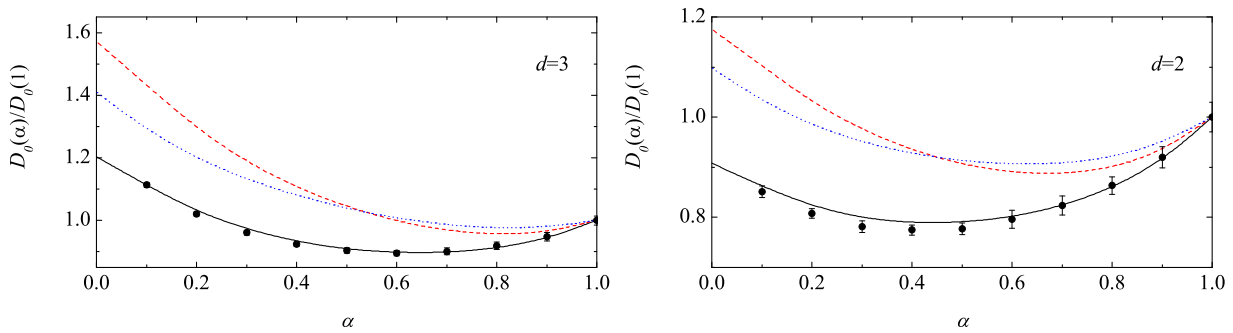


FIG. 4: (color online) Plot of the reduced kinetic diffusion coefficient $D_0(\alpha)/D_0(1)$ as a function of the (common) coefficient of restitution $\alpha = \alpha_0$ for $m_0/m = 1/8$, $\sigma_0/\sigma = 1/2$ and $\phi = 0$. The left panel is for hard spheres ($d = 3$) while the right panel is for hard disks ($d = 2$). The solid lines correspond to the second Sonine approximation, the dashed lines refer to the first Sonine approximation and the dotted lines are the modified Sonine approximation. The symbols are the results obtained from Monte Carlo simulations. Here, $D_0(1)$ is the elastic value of the thermal diffusion coefficient consistently obtained in each approximation.

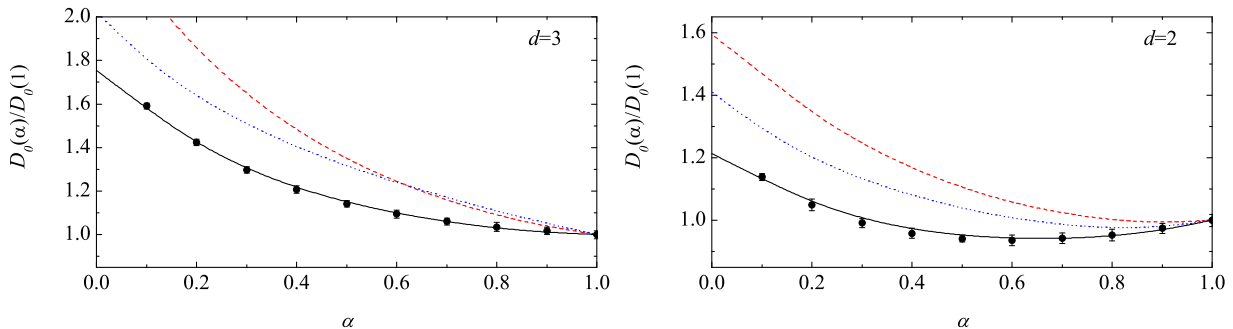


FIG. 5: (color online) Plot of the reduced kinetic diffusion coefficient $D_0(\alpha)/D_0(1)$ as a function of the (common) coefficient of restitution $\alpha = \alpha_0$ for $m_0/m = 1/5$, $\sigma_0/\sigma = 1/2$ and $\phi = 0.2$. The left panel is for hard spheres ($d = 3$) while the right panel is for hard disks ($d = 2$). The solid lines correspond to the second Sonine approximation, the dashed lines refer to the first Sonine approximation and the dotted lines are the modified Sonine approximation. The symbols are the results obtained from Monte Carlo simulations. Here, $D_0(1)$ is the elastic value of the thermal diffusion coefficient consistently obtained in each approximation.

is the (reduced) cooling rate and the reduced quantities X_1^* , Y_1^* and ν_1^* are given by Eqs. (B15), (B21) and (C1), respectively.

In general, the first and second Sonine approximations for the transport coefficients of the mass flux have a complex dependence on the coefficients of restitution, the solid fraction and the mass and size ratios. Thus, before analyzing this dependence, it is instructive to consider some special limits. In the elastic limit ($\alpha = \alpha_0 = 1$) of a three-dimensional system, one recovers previous results for a gas mixture of elastic hard spheres [39, 40]. Moreover, in the case of mechanically equivalent particles ($m_0 = m$, $\sigma_0 = \sigma$, $\alpha = \alpha_0$), as expected, one gets $D^T[2] = 0$, $D_0[2] = -(m/x_0 m_0)D[2]$, and so

$$\mathbf{j}_0^{(1)} = -\frac{nm_0^2}{\rho}D_0[2]\nabla x_0, \quad (49)$$

where $x_0 = n_0/n$ is the mole fraction of impurities. Moreover, in the case of a dilute gas ($\phi = 0$), the expression of the kinetic diffusion coefficient $D_0[2]$ coincides with the one previously derived by one of the authors [20] by assuming that the solvent is in the homogeneous cooling state. All these results confirm the self-consistency of the results reported in this paper.

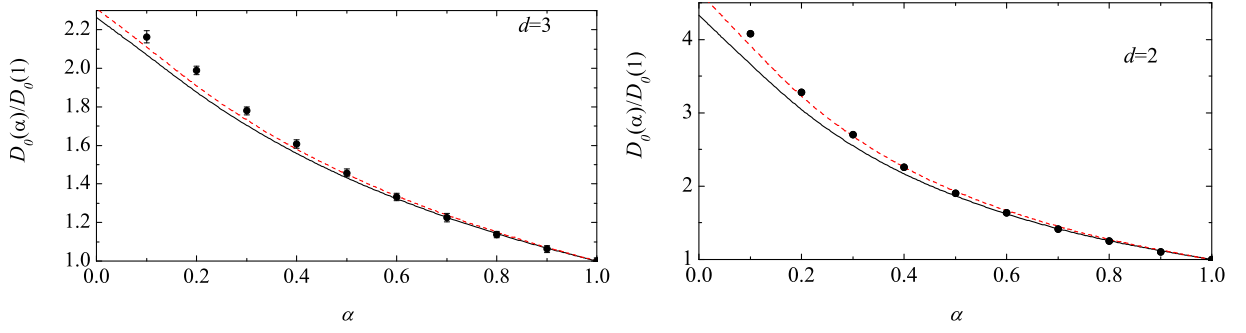


FIG. 6: (color online) Plot of the reduced kinetic diffusion coefficient $D_0(\alpha)/D_0(1)$ as a function of the (common) coefficient of restitution $\alpha = \alpha_0$ for $m_0/m = 2$, $\sigma_0/\sigma = 2$ and $\phi = 0.2$. The left panel is for hard spheres ($d = 3$) while the right panel is for hard disks ($d = 2$). The solid lines correspond to the second Sonine approximation and the dashed lines refer to the first Sonine approximation. The symbols are the results obtained from Monte Carlo simulations. Here, $D_0(1)$ is the elastic value of the thermal diffusion coefficient consistently obtained in each approximation.

V. SOME ILLUSTRATIVE EXAMPLES AND COMPARISON WITH MONTE CARLO SIMULATIONS

The expressions (42)–(44) for the (reduced) transport coefficients $D_0[2]/D_0[1]$, $D[2]/D[1]$ and $D^T[2]/D^T[1]$ depend on many parameters: $\{m_0/m, \sigma_0/\sigma, \alpha, \alpha_0, \phi\}$, or equivalently [11] $\{m_0^*/m, \sigma_0/\sigma, \alpha, \phi\}$, where m_0^* is defined by Eq. (14). This complexity exists in the elastic limit as well [4], except for the dependence on the coefficients of restitution. Thus, to show more clearly the influence of dissipation on the transport coefficients we normalize them with respect to their values in the elastic limit. Also, for simplicity, we take the simplest case of common coefficient of restitution $\alpha = \alpha_0$ so that, the parameter space has four independent quantities: $\{m_0/m, \sigma_0/\sigma, \alpha, \phi\}$.

In order to get the explicit dependence of the transport coefficients on the above four parameters one has to give the forms of the pair correlation functions $\chi^{(0)}$ and $\chi_0^{(0)}$. In the three-dimensional case ($d = 3$), a good approximation for $\chi^{(0)}$ is provided by the Carnahan-Starling form [41]

$$\chi^{(0)} = \frac{1 - \frac{1}{2}\phi}{(1 - \phi)^3}, \quad (50)$$

while the intruder-gas pair correlation function is given by [42]

$$\chi_0^{(0)} = \frac{1}{1 - \phi} + 3\frac{\omega}{1 + \omega} \frac{\phi}{(1 - \phi)^2} + 2\frac{\omega^2}{(1 + \omega)^2} \frac{\phi^2}{(1 - \phi)^3}, \quad (51)$$

where we recall that $\omega = \sigma_0/\sigma$ is the diameter ratio. The expression for the chemical potential of the intruder consistent with the approximation (51) is [43]

$$\begin{aligned} \frac{\mu_0}{T} = & C_3 + \ln n_0 - \ln(1 - \phi) + 3\omega \frac{\phi}{1 - \phi} + 3\omega^2 \left[\ln(1 - \phi) + \frac{\phi(2 - \phi)}{(1 - \phi)^2} \right] \\ & - \omega^3 \left[2\ln(1 - \phi) + \frac{\phi(1 - 6\phi + 3\phi^2)}{(1 - \phi)^3} \right], \end{aligned} \quad (52)$$

where C_3 is a constant. For a two-dimensional gas ($d = 2$), $\chi^{(0)}$ and $\chi_0^{(0)}$ are approximately given by [44]

$$\chi^{(0)} = \frac{1 - \frac{7}{16}\phi}{(1 - \phi)^2}, \quad (53)$$

$$\chi_0^{(0)} = \frac{1}{1 - \phi} + \frac{9}{8} \frac{\omega}{1 + \omega} \frac{\phi}{(1 - \phi)^2}. \quad (54)$$

The chemical potential is now given by [45]

$$\frac{\mu_0}{T} = C_2 + \ln n_0 - \ln(1 - \phi) + \frac{1}{4}\omega \left[\frac{9\phi}{1 - \phi} + \ln(1 - \phi) \right] + \frac{1}{8}\omega^2 \left[\frac{\phi(7 + 2\phi)}{(1 - \phi)^2} - \ln(1 - \phi) \right], \quad (55)$$

where C_2 is a constant.

In Figs. 1–3, we plot the transport coefficients for inelastic hard spheres ($d = 3$) as functions of the coefficient of restitution for two different systems. Each transport coefficient has been reduced with respect to its elastic value consistently obtained in each approximation. The dashed lines refer to the first Sonine approximation while the solid lines correspond to the second Sonine approximation. We observe that in general the first Sonine polynomial approximation quantitatively differs from the second Sonine approach as the dissipation increases for sufficiently small values of the mass ratio m_0/m and/or the size ratio σ_0/σ . For these cases, the first Sonine approximation is not sufficient to capture the influence of dissipation on mass transport. However, the predictions of the first Sonine correction improve significantly as m_0/m and/or σ_0/σ increases so that the former accurately describes the mass transport in this range of values of the mass and size ratios, even for strong inelasticity. These findings on the convergence of the Sonine polynomial expansion are quite similar to those obtained for elastic systems [40] and for granular gases at low-density [20].

To check the reliability of the first and second Sonine approximations, we have performed Monte Carlo simulations of the Enskog equation for the dense granular gas with the tracer particles. We have extracted from these simulations the kinetic diffusion coefficient D_0 of impurities in a granular dense gas in the homogeneous cooling state (HCS). This coefficient can be obtained from the mean square displacement of the intruder particle after a time interval t as [20, 46]

$$\frac{\partial}{\partial t} \langle |\mathbf{r}(t) - \mathbf{r}(0)|^2 \rangle = \frac{2dD_0}{n}, \quad (56)$$

where $|\mathbf{r}(t) - \mathbf{r}(0)|$ is the distance travelled by the intruder from $t = 0$ until time t . Equation (56) is the Einstein form of the diffusion coefficient. This relation can be used also in Monte Carlo simulations of granular gases to measure the diffusion coefficient (see for example a previous work on transport of impurities in a dilute granular gas in Ref. [20]). In an unbounded system like ours, the DSMC method has two steps that are repeated in each time iteration: the first step takes care of the particles drift and the second step accounts for the collisions among particles. The extension of the DSMC method to study the diffusion of impurities in a dense granular gas in the HCS requires the changes $J[f, f] \rightarrow \chi J[f, f]$ and $J_0[f_0, f] \rightarrow \chi_0 J_0[f_0, f]$. For the DSMC method to work appropriately, the time step needs to be small in comparison with the microscopic time scale of the problem (which is set by the collision frequency ν) and we also need a sufficiently high number of simulated particles [33]. Thus, we have used in the simulations of this work a time step $\delta t = 2.5 \times 10^{-4} \nu^{-1}$ and $N = 2 \times 10^6$ simulated particles for each species [47]. To our knowledge and since we are interested in the complete range of values of α , we present the first DSMC data on dense granular gases for coefficients of restitution as low as $\alpha = 0.1$. More details on the application of the DSMC method [33] to this diffusion problem can be found in Ref. [20].

If a hydrodynamic description (or normal solution in the context of the CE method) applies, then the diffusion coefficient $D_0(t)$ depends on time only through its dependence on the temperature $T(t)$. In this case, after a transient regime, the reduced diffusion coefficient $D_0(\alpha)/D_0(1)$ achieves a time-independent value [20]. Here, we compare the steady state values of $D_0(\alpha)/D_0(1)$ obtained from Monte Carlo simulations with the theoretical predictions given by the first and second Sonine approximations.

Let us consider first the dilute gas limit ($\phi = 0$). Figure 4 shows the reduced diffusion coefficient $D_0(\alpha)/D_0(1)$ for $m_0/m = 1/8$ and $\sigma_0/\sigma = 1/2$ for disks ($d = 2$) and spheres ($d = 3$). According to the theory results obtained in the previous figures, one expects that in the Lorentz gas limit (small values of the mass and size ratios) both Sonine approximations differ significantly for strong inelasticity (this means obviously that it is not possible that both of them simultaneously show good agreement with the exact solution of the problem). For the sake of completeness, we have also included the results recently derived for binary mixtures [25] from a new method based on a modified version of the first Sonine approximation which replaces the Maxwell-Boltzmann distribution weight function (used in the standard Sonine approximations) by the homogeneous cooling state distribution [25, 48]. This new method partially eliminates the observed disagreement (for strong dissipation) between computer simulations [49] and theoretical results for the heat flux transport coefficients [25]. The explicit expression for the coefficient D_0 obtained from the modified Sonine method is displayed in Appendix D. The simulation data corresponding to $d = 3$ for $\alpha \geq 0.5$ were reported in Ref. [20] while those corresponding to $d = 2$ and $d = 3$ for $\alpha \leq 0.5$ have been obtained in this work. It is quite apparent that while the second Sonine approximation agrees very well with simulation data, the standard and modified first Sonine approximations fail for strong dissipation. This agreement is specially significant in the case of hard spheres. Thus, as expected, the Sonine polynomial expansion exhibits a poor convergence for sufficiently small values of the mass and size ratios. To assess the influence of density on these trends, the ratio $D_0(\alpha)/D_0(1)$ is plotted in Fig. 5 for $m_0/m = 1/5$, $\sigma_0/\sigma = 1/2$ in the case of a moderately dense gas ($\phi = 0.2$). As before, both first Sonine approximations underestimate the diffusion coefficient (the discrepancy being more important in the case of the standard than the modified first Sonine approximation) while the predictions of the second Sonine approach show an excellent agreement with simulation data in the whole range of values of the coefficient of restitution. All these results clearly confirm the

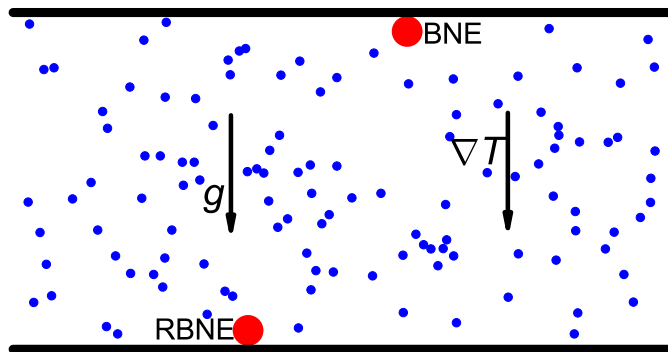


FIG. 7: (color online) Sketch of the segregation problem analyzed in Sec. VI. The small circles represent the particles of the dense gas while the large circles are the intruders. The BNE (RBNE) effect corresponds to the situation in which the intruder rises (falls) to the top (bottom) plate.

accuracy of the second Sonine approximation, even for low values of α and small values of the mass and size ratios. Figure 6 shows that in the opposite limit of large values of the mass and size ratios (Rayleigh gas limit), the first and second Sonine approximations are practically indistinguishable for moderately large inelasticity (say for instance, $\alpha \geq 0.5$) and both approaches provide a general good agreement with Monte Carlo simulations. However, at very high inelasticity, the second Sonine approximation very slightly underestimates the diffusion coefficient compared to the DSMC data and the first Sonine approximation. We have performed more series of simulations (not shown here) with different values of the ratios m_0/m and σ_0/σ confirming similar trends as those in the figures shown in this Section for both cases $m_0/m < 1$ and/or $\sigma_0/\sigma < 1$ and $m_0/m > 1$ and/or $\sigma_0/\sigma > 1$ (the data are available to the reader upon request to the authors).

VI. SEGREGATION BY THERMAL DIFFUSION

As an application of the previous results, this Section is devoted to the study of segregation, driven by both gravity and temperature gradients, of an intruder in a granular dense gas. Segregation and mixing of dissimilar grains is one of the most interesting problems in granular mixtures not only from a fundamental point of view but also from a more practical point of view. This problem has spawned a number of important experimental, computational and theoretical works in the field of granular media [50]. Although several mechanisms have been proposed in the literature, the problem is not completely understood yet. Among the different mechanisms, thermal diffusion becomes the most relevant if the system resembles the conditions of a granular gas. In this case, kinetic theory tools have proven to be quite useful to analyze the motion of the intruder. A short previous analysis on this problem, but when the system is heated by a stochastic-driving force, has been reported in Ref. [32].

Thermal diffusion is caused by the relative motion of the components of a mixture due to the presence of a temperature gradient. As a result of this motion, a steady state is finally reached in which the separating effect arising from thermal diffusion is balanced by the remixing effect of ordinary diffusion [51]. Under these conditions, the thermal diffusion factor Λ characterizes the amount of segregation parallel to the temperature gradient. Our goal here is to determine Λ in a non-convecting ($\mathbf{u} = \mathbf{0}$) steady state with gradients only in the vertical direction (z axis) for simplicity. In this case, Λ is defined as

$$-\Lambda \partial_z \ln T = \partial_z \ln \left(\frac{n_0}{n} \right). \quad (57)$$

If we assume that gravity and thermal gradient point in parallel directions (i.e., the bottom plate is hotter than the top plate), then the intruder rises with respect to the fluid particles if $\Lambda > 0$ while the intruder falls with respect to the fluid particles if $\Lambda < 0$. If the impurity is heavier than the gas particles, the former situation is referred to as the Brazil-nut effect (BNE) while the latter is called the reverse Brazil-nut effect (RBNE). A sketch of the geometry of the segregation problem studied here is given in Fig. 7. The key point here is that logically the segregation condition (57) will depend on the mass flux transport coefficients of the intruder. We remind the reader of the features, some of them described in the Introduction, that the transport coefficients we use here are able to capture (compared to alternative coefficients in theoretical works on segregation by other authors [29, 30]). These features are a consequence of the consistent development of the Chapman-Enskog theory for dense granular mixtures [14]. Due to this, and in addition to the gain of accuracy with the use of the second order term in the Sonine expansion, we expect that our

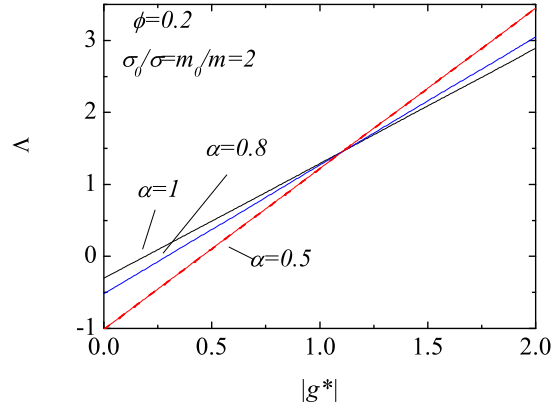


FIG. 8: (color online) Plot of the thermal diffusion factor Λ versus the (reduced) gravity $|g^*|$ for $\phi = 0.2$ and three values of the (common) coefficient of restitution α : $\alpha = 1, 0.8$ and 0.5 .

expressions (45)-(47) will be useful in practical problems and applications of granular segregation [53]. We determine below the explicit expression of this segregation criterion.

As said before, let us consider a steady base state with no flow ($\mathbf{u} = \mathbf{0}$) and with a temperature gradient parallel to the direction of gravity (in this case, the z direction). According to Eq. (16), the mass flux \mathbf{j}_0 vanishes in this state (because $\mathbf{u} = \mathbf{0}$) and there are no contributions to the pressure tensor except for those coming from the hydrostatic pressure term, i.e., $P_{ij} = p\delta_{ij}$, where p is given by Eq. (30). As a consequence, the momentum balance equation (9) becomes

$$\frac{\partial p}{\partial z} = \frac{\partial p}{\partial T} \partial_z T + \frac{\partial p}{\partial n} \partial_z n = -\rho g. \quad (58)$$

Finally, the constitutive equation for the mass flux is given by Eq. (1) with $\nabla \rightarrow \partial_z$. Using the fact that $j_{0,z} = 0$ and taking into account Eqs. (1) and (57), the factor Λ can be written as

$$\Lambda = \frac{\beta D^{T*} - (p^* + g^*)(D_0^* + D^*)}{\beta D_0^*}, \quad (59)$$

where we have introduced the reduced transport coefficients $D^{T*} = (\rho\nu/n_0T)D^T$, $D_0^* = (m_0^2\nu/\rho T)D_0$, and $D^* = (m_0\nu/n_0T)D$. Moreover, $p^* = p/nT = 1 + 2^{d-2}(1 + \alpha)\chi^{(0)\phi}$,

$$\beta = p^* + \phi \partial_\phi p^* = 1 + 2^{d-2}(1 + \alpha)\chi^{(0)\phi} \left[1 + \phi \frac{\partial}{\partial \phi} \ln(\phi\chi^{(0)}) \right] \quad (60)$$

and

$$g^* = \frac{\rho g}{n \left(\frac{\partial T}{\partial z} \right)} < 0 \quad (61)$$

is a dimensionless parameter measuring the gravity relative to the thermal gradient. This parameter measures the competition between these two mechanisms (g and $\partial_z T$) on segregation.

As expected, the dependence of Λ on the parameter space of the problem is quite intricate. Regarding the dependence of thermal diffusion on gravity, we observe that for given values of the mass and size ratios, the coefficient of restitution and density, it is possible to switch between RBNE ($\Lambda < 0$) and BNE ($\Lambda > 0$) by changing the value of gravity relative to the thermal gradient. This is a new interesting effect not captured in previous works on segregation [29, 30, 52]. As an illustration of this effect, Fig. 8 presents plots of the second Sonine approximation for Λ as a function of the (reduced) gravity for a three-dimensional system with $\phi = 0.2$, $\sigma_0/\sigma = m_0/m = 2$ and three different values of the (common) coefficient of restitution α . It is apparent that, for the case analyzed here, the RBNE is dominant at small values of $|g^*|$ while the opposite happens as the dimensionless gravity increases.

The condition $\Lambda = 0$ provides the segregation criterion for the transition BNE \Leftrightarrow RBNE. Since β and D_0^* are positive, then, according to (59), $\text{sgn}(\Lambda) = \text{sgn}(\beta D^{T*} - (p^* + g^*)(D_0^* + D^*))$. As a consequence, the segregation criterion is

$$\beta D^{T*} = (p^* + g^*)(D_0^* + D^*). \quad (62)$$

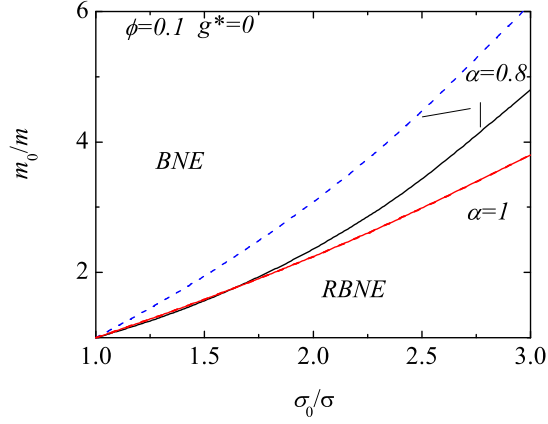


FIG. 9: (color online) Phase diagram for BNE/RBNE for $\phi = 0.1$ in the absence of gravity and for two values of the (common) coefficient of restitution α . Points above the curve correspond to $\Lambda > 0$ (BNE) while points below the curve correspond to $\Lambda < 0$ (RBNE). The dashed line is the result obtained from the first Sonine approximation for $\alpha = 0.8$.

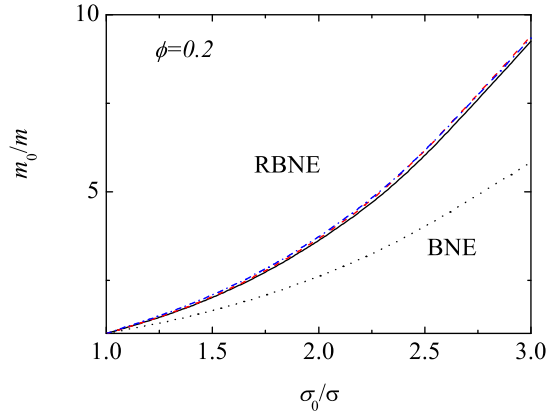


FIG. 10: (color online) Phase diagram for BNE/RBNE for $\phi = 0.2$ in the absence of thermal gradient ($|g^*| \rightarrow \infty$) for three values of α : $\alpha = 1, 0.8$ (dashed line) and 0.5 (dashed-dotted line). The dotted line refers to the results obtained by Jenkins and Yoon [29] for an elastic system.

As expected, when $m_0 = m$, $\sigma_0 = \sigma$ and $\alpha = \alpha_0$, the system (intruder plus gas) is monodisperse and the two species do not segregate. This is consistent with Eq. (62) since in this limit case $D^{T*} = D_0^* + D^* = 0$ so that $\Lambda = 0$ for any value of α and ϕ . On the other hand, in the case of a dilute gas ($\phi = 0$), one has $\beta = p^* = 1$ and the condition (62) when $g^* = 0$ in the first Sonine approximation becomes

$$\frac{m_0}{m} = \frac{T_0}{T}. \quad (63)$$

This segregation condition agrees with some recent results derived from the Boltzmann equation [31, 54]. It must be remarked that, due to the lack of energy equipartition, the condition $m_0/m = T_0/T$ is rather complicated since it involves all the parameters of the system.

We consider now dense systems. For the sake of concreteness, we assume that the intruder is larger than the gas particles ($\sigma_0 > \sigma$). Figure 9 shows a phase-diagram in the $(m_0/m, \sigma_0/\sigma)$ -plane for a moderate dense gas ($\phi = 0.1$) in the absence of gravity and two values of the coefficient of restitution. Also, for comparison the corresponding phase-diagram obtained from the first Sonine approximation is plotted for the case $\alpha = 0.8$. We observe that, in the absence of gravity, the main effect of dissipation is to reduce the size of the BNE. This conclusion qualitatively agrees with the results derived in the driven gas case [32]. However, at a quantitative level, the influence of dissipation observed here is less important than the one obtained in the heated case. Moreover, although the first Sonine approximation reproduces qualitatively the trends of the phase-diagram, the former overestimates the predictions of the second Sonine approximation, especially when increasing the mass and size ratios.

In some previous theoretical studies [29, 30, 52], it has been assumed that the global temperature of the bed does

not vary with height so that the effect of $\partial_z T$ on segregation is neglected. In this limit ($|g^*| \rightarrow \infty$), the condition (62) reduces to $D_0^* + D^* = 0$. The form of the phase diagram in the limit $|g^*| \rightarrow \infty$ is shown in Fig. 10 for $\phi = 0.2$ and three values of the coefficient of restitution. The result derived by Jenkins and Yoon [29] in the elastic case from a simple kinetic theory (namely, just a particular case from the perspective of the theory presented in this work) has also been included for comparison. In contrast to the case $g^* = 0$, we observe that the RBNE regime appears essentially now for both large mass ratio and/or small size ratio. With respect to the influence of inelasticity, Fig. 10 shows that the phase diagram is practically independent of the value of the coefficient of restitution since the three curves collapse in a common curve. We also observe that our results differ from those obtained by Jenkins and Yoon [29], especially for large size ratios.

VII. CONCLUSIONS

In this paper we have analyzed the mass transport of impurities in a moderately dense granular gas described by the inelastic Enskog kinetic equation. This is perhaps the simplest example of transport in a *multicomponent* granular gas since the tracer particles (impurities) are enslaved to the granular gas (solvent) and there are fewer parameters. Nevertheless, it involves, as we explained, many situations of practical interest in the study of granular gases. In the tracer limit, once the state of the solvent is well characterized, the mass flux \mathbf{j}_0 associated with impurities is the relevant flux of the problem. To first order in the spatial gradients, \mathbf{j}_0 is given by Eq. (1) where D_0 is the kinetic diffusion coefficient, D is the mutual diffusion coefficient and D^T is the thermal diffusion coefficient.

The main goal of this paper has been to determine these three transport coefficients as functions of the temperature, the density and the different mechanical parameters of the system, namely, the masses and particle diameters and the (constant) coefficients of restitution for the impurity-gas and gas-gas collisions. Like for elastic collisions [4], the coefficients D_0 , D and D^T are given in terms of the solutions of a set of coupled linear integral equations [14]. A practical evaluation of the above diffusion coefficients is possible by using a Sonine polynomial expansion and approximate results are not limited to weak inelasticity. Here, D_0 , D and D^T have been determined in the first (one polynomial) and second (two polynomials) Sonine approximation and progress was possible here thanks to previous results obtained by using the (standard) first Sonine approximation [15] for the full Navier-Stokes transport coefficients of polydisperse dense mixtures. The present study complements and extends previous works on diffusion in granular dilute [20] and dense [55] gases and provides explicit expressions for D_0 , D and D^T beyond the first Sonine approximation [15].

Comparison of the theoretical results derived for D_0 , D and D^T between the first and second Sonine approximations shows significant discrepancies between both approaches for values of the mass ratio m_0/m and/or the size ratio σ_0/σ smaller than 1 while the quality of the first Sonine correction improves with increasing values of m_0/m and σ_0/σ . These trends are quite similar to those previously found for tracer diffusion in an ordinary (elastic) dense gas [40] and in a granular dilute gas [20]. Moreover, to check to reliability of the different theoretical approaches, a comparison with Monte Carlo simulations of the Enskog equation for the coefficient D_0 has been carried out for disks ($d = 2$) and spheres ($d = 3$). The comparison with simulation data shows the superiority of the second Sonine approximation over other approaches (the standard first Sonine approximation and a modified version of the first Sonine correction recently proposed [25, 48]), since the agreement of D_0 [2] with numerical results is excellent, even for strong dissipation (see for instance Figs. 4 and 5) and very small values of the mass and size ratios.

With respect to the segregation problem, which has of growing interest in the research community in the field, we have shown that the explicit knowledge of the three diffusion coefficients allows one to compute the thermal diffusion factor Λ . This quantity provides a convenient measure of the separation or segregation generated by a temperature gradient in a multicomponent system. According to the symmetry of the problem (sketched in Fig. 7), when $\Lambda > 0$ the intruder tends to climb to the top of the sample against gravity (Brazil-nut effect, BNE) while if $\Lambda < 0$ the intruder tends to move at the bottom of the system (reverse Brazil-nut effect, RBNE). The understanding of the transition BNE/RBNE is of central interest in the field of granular matter mainly due to its practical/industrial importance. The analysis carried out here provides an extension of a previous analysis [32] for a heated dense gas in the first Sonine approximation. Our results show that the influence of dissipation on the phase diagram BNE/RBNE is much more significant in the absence of gravity ($|g^*| = 0$) than in the opposite limit ($|g^*| = \infty$). In fact, as Fig. 10 shows, when the segregation of the intruder is essentially driven by gravity, the inelasticity of collisions has not discernible influence on the form of the phase diagram BNE/RBNE. From the discussion in previous Sections, we expect the segregation criteria presented here to be more accurate in comparison with the criteria derived in other works [29, 30]. Future research work using a DSMC code adapted to the problem of segregation, molecular dynamics (MD) simulations, and eventually, experiments, will help us to test our theory (and previous alternative theories) in real problems. We are currently working on DSMC and MD simulations.

An important issue is the usefulness of the expressions for the NS transport coefficients derived here. As already

said in a previous work [25], the NS hydrodynamic equations themselves may or may not be limited with respect to inelasticity, depending on the particular granular flow considered. In particular, tracer diffusion in the HCS at very low values of the coefficient of restitution is only possible for very small systems due to the spontaneous formation of velocity vortices and density clusters. Moreover, in most of problems of practical interest (such as steady states for a granular gas heated or sheared from the boundaries), the strength of spatial gradients is set by inelasticity so that the NS description only holds in the quasielastic limit [56]. Nevertheless, in spite of the above cautions, the NS equations are still appropriate for a wide class of flows. Some of them correspond to the stability analysis of small perturbations of the HCS [57], supersonic flows past a wedge [58] and hydrodynamic profiles of systems vibrated vertically [59] where comparisons between theory and experiments have shown both qualitative and quantitative agreement for moderate values of dissipation (say for instance, $\alpha \gtrsim 0.8$). Consequently, the NS equations with the transport coefficients derived here can be considered still as an useful theory for a wide class of rapid granular flows, although more limited than for ordinary gases.

One of the main limitations of the present study is its restriction to the tracer or intruder limit. This precludes the possibility of analyzing the influence of composition on the mass transport. The extension of the results derived here to finite mole fractions is an interesting open problem. Moreover, it would also be interesting to evaluate the expressions for the remaining transport coefficients of the mixture (shear viscosity, bulk viscosity, thermal conductivity, ...) for a variety of mass and diameter ratios. This evaluation would allow one to assess the quality of the approximate Sonine method for solving the integral equations for the transport coefficients through a comparison with computer simulations. Previous results obtained for the shear viscosity coefficient [19] have shown a good agreement. Moreover, the knowledge of the full NS transport coefficients for a dense granular binary mixture allows us to determine the dispersion relations for the hydrodynamic equations linearized about the homogeneous cooling state. Some previous results [60] based on the Boltzmann kinetic equation have shown that the resulting equations exhibit a long wavelength instability for three of the modes. The objective now is to extend to higher densities this previous linear stability analysis for a dilute gas [60] and compare the theoretical predictions with MD simulations for the homogenous cooling state. We plan to carry out such studies in the near future.

Acknowledgments

We are grateful to Andrés Santos for useful comments on an early version of this paper. This research has been supported by the Ministerio de Educacion y Ciencia (Spain) through Programa Juan de la Cierva (F.V.R.) and Grant No. FIS2007-60977. Partial support from the Junta de Extremadura through Grant No. GRU07046 is also acknowledged.

APPENDIX A: FIRST ORDER VELOCITY DISTRIBUTION FUNCTION OF THE GAS

The first order velocity distribution function $f^{(1)}$ of the gas particles has the form [16, 17]

$$f^{(1)} = \mathcal{A} \cdot \nabla T + \mathcal{C} \cdot \nabla n + \mathcal{D} : \nabla \mathbf{u} + E \nabla \cdot \mathbf{u}. \quad (\text{A1})$$

Only the coefficients \mathcal{A} and \mathcal{C} are involved in the evaluation of the mass transport $\mathbf{j}_0^{(1)}$ of the intruder. These quantities verify the linear integral equations [9, 17]

$$\frac{1}{2} \zeta^{(0)} \frac{\partial}{\partial \mathbf{V}} \cdot (\mathbf{V} \mathcal{A}) - \frac{1}{2} \zeta^{(0)} \mathcal{A} - \left(J^{(0)}[\mathcal{A}, f^{(0)}] + J^{(0)}[f^{(0)}, \mathcal{A}] \right) = \mathbf{A}, \quad (\text{A2})$$

$$\frac{1}{2} \zeta^{(0)} \frac{\partial}{\partial \mathbf{V}} \cdot (\mathbf{V} \mathcal{C}) - n \frac{\partial \zeta^{(0)}}{\partial n} \mathcal{A} - \left(J^{(0)}[\mathcal{C}, f^{(0)}] + J^{(0)}[f^{(0)}, \mathcal{C}] \right) = \mathbf{C}, \quad (\text{A3})$$

where $J^{(0)}[X, Y]$ is the linearized collision operator

$$J^{(0)}[\mathbf{v}_1 | X, Y] = \chi^{(0)} \sigma^{d-1} \int d\mathbf{v}_2 \int d\hat{\boldsymbol{\sigma}} \Theta(\hat{\boldsymbol{\sigma}} \cdot \mathbf{g})(\hat{\boldsymbol{\sigma}} \cdot \mathbf{g}) \left[\alpha^{-2} X(\mathbf{V}_1'') Y(\mathbf{V}_2'') - X(\mathbf{V}_1) Y(\mathbf{V}_2) \right], \quad (\text{A4})$$

and the inhomogeneous terms of the integral equations (A2) and (A3) are defined by

$$A_i(\mathbf{V}) = \frac{1}{2} V_i \frac{\partial}{\partial \mathbf{V}} \cdot (\mathbf{V} f^{(0)}) - \frac{p}{\rho} \frac{\partial}{\partial V_i} f^{(0)} + \frac{1}{2} \mathcal{K}_i \left[\frac{\partial}{\partial \mathbf{V}} \cdot (\mathbf{V} f^{(0)}) \right], \quad (\text{A5})$$

$$C_i(\mathbf{V}) = -\mathbf{V}f^{(0)} - m^{-1} \frac{\partial}{\partial V_i} f^{(0)} \frac{\partial p}{\partial n} - \left(1 + \frac{1}{2} \phi \frac{\partial \ln \chi^{(0)}}{\partial \phi}\right) \mathcal{K}_i [f^{(0)}]. \quad (\text{A6})$$

Here, the operator $\mathcal{K}_i[X]$ is given by

$$\mathcal{K}_i[X] = \sigma^d \chi^{(0)} \int d\mathbf{v}_2 \int d\hat{\boldsymbol{\sigma}} \Theta(\hat{\boldsymbol{\sigma}} \cdot \mathbf{g})(\hat{\boldsymbol{\sigma}} \cdot \mathbf{g}) \hat{\sigma}_i \left[\alpha^{-2} f^{(0)}(\mathbf{V}'_1) X(\mathbf{V}'_2) + f^{(0)}(\mathbf{V}_1) X(\mathbf{V}_2) \right].$$

The functions \mathcal{A} and \mathcal{C} are zero in the first Sonine approximation [16, 17]. In the second Sonine approximation, these quantities are given by

$$\mathcal{A}(\mathbf{V}) \rightarrow -f_M(\mathbf{V})a \mathbf{S}(\mathbf{V}), \quad \mathcal{C}(\mathbf{V}) \rightarrow -f_M(\mathbf{V})c \mathbf{S}(\mathbf{V}), \quad (\text{A7})$$

where

$$f_M(\mathbf{V}) = n \left(\frac{m}{2\pi T} \right)^{d/2} \exp\left(-\frac{mV^2}{2T}\right), \quad (\text{A8})$$

and

$$\mathbf{S}(\mathbf{V}) = \left(\frac{1}{2}mV^2 - \frac{d+2}{2}T \right) \mathbf{V}. \quad (\text{A9})$$

Substitution of (A7) into Eqs. (A2) and (A3) gives a set of closed equations for a and c . Multiplication of these equations by $\mathbf{S}(\mathbf{V})$ and integration over \mathbf{V} yields a set of algebraic equations whose solution is [16, 17]

$$a = \frac{1 + 3 \frac{2^{d-3}}{d+2} \phi \chi^{(0)} (1 + \alpha)^2 (2\alpha - 1)}{\nu T^2 (\nu_\kappa^* - 2\zeta^*)}, \quad (\text{A10})$$

$$c = \frac{1}{nT\nu} \left(\nu_\kappa^* - \frac{3}{2}\zeta^* \right)^{-1} \left[aT^2 \nu \frac{\xi \zeta^*}{\chi^{(0)}} - 3 \frac{2^{d-3}}{d+2} \phi (\chi^{(0)} + \xi) \alpha (1 - \alpha^2) \right], \quad (\text{A11})$$

where $\nu = n\sigma^{d-1} \sqrt{2T/m}$, ζ^* is given by (48),

$$\xi \equiv \frac{\partial}{\partial \phi} \left(\phi \chi^{(0)} \right) \quad (\text{A12})$$

and

$$\nu_\kappa^* = \frac{8}{d(d+2)} \frac{\pi^{(d-1)/2}}{\sqrt{2}\Gamma(d/2)} \chi^{(0)} (1 + \alpha) \left[\frac{d-1}{2} + \frac{3}{16}(d+8)(1-\alpha) \right]. \quad (\text{A13})$$

It must be remarked that all the above expressions have been obtained by neglecting some non-Gaussian contributions to the zeroth-order distribution $f^{(0)}$. The influence of these non-Gaussian terms is only significant for quite extreme values of dissipation [49].

APPENDIX B: FIRST AND SECOND SONINE APPROXIMATIONS FOR THE MASS FLUX OF IMPURITIES

In this Appendix we determine the transport coefficients D_0 , D and D^T associated with the mass flux in the first and second Sonine approximation. In this case, the functions \mathcal{A}_0 , \mathcal{B}_0 and \mathcal{C}_0 are given by Eqs. (34)–(36), respectively while \mathcal{A} and \mathcal{C} are approximated by (A7). Let us start with the thermal diffusion coefficient D^T , which is defined by Eq. (20). To get it, we substitute first \mathcal{A}_0 and \mathcal{A} by their Sonine approximations (34) and (A7), respectively, and then we multiply the integral equation (23) by $m_0 \mathbf{V}$ and integrate over velocity. After some algebra, the result is

$$(\nu_1 - \zeta^{(0)})D^T + \frac{n_0 T_0^2}{\rho} \nu_2 a_0 = Z_1, \quad (\text{B1})$$

where

$$Z_1 = -\frac{x_0 T_0^2}{m} \nu_3 a - \frac{x_0 p m_0}{m \rho} \left(1 - \frac{\rho T_0}{m_0 p}\right) - \frac{1}{2d\rho} \int d\mathbf{v} m_0 V_i \mathcal{K}_{0,i} \left[\frac{\partial}{\partial \mathbf{V}} \cdot (\mathbf{V} f^{(0)}) \right], \quad (\text{B2})$$

and we have introduced the collision frequencies

$$\nu_1 = -\frac{1}{dn_0 T_0} \int d\mathbf{v} m_0 \mathbf{V} \cdot J_0^{(0)} [f_{0,M} \mathbf{V}, f^{(0)}], \quad (\text{B3})$$

$$\nu_2 = -\frac{1}{dn_0 T_0^2} \int d\mathbf{v} m_0 \mathbf{V} \cdot J_0^{(0)} [f_{0,M} \mathbf{S}_0, f^{(0)}], \quad (\text{B4})$$

$$\nu_3 = -\frac{1}{dn_0 T_0^2} \int d\mathbf{v} m_0 \mathbf{V} \cdot J_0^{(0)} [f_0^{(0)}, f_M \mathbf{S}]. \quad (\text{B5})$$

The operator $\mathcal{K}_{0,i}[X]$ is defined in Eq. (32). The collision integral appearing on the right-hand side of Eq. (B2) involving this operator has been evaluated in Ref. [15] with the result

$$\frac{1}{2d\rho} \int d\mathbf{v} m_0 V_i \mathcal{K}_{0,i} \left[\frac{\partial}{\partial \mathbf{V}} \cdot (\mathbf{V} f^{(0)}) \right] = -\frac{1}{2} \frac{x_0 T}{m} (1 + \omega)^d M_0 \phi \chi_0^{(0)} (1 + \alpha_0), \quad (\text{B6})$$

where $\omega \equiv \sigma_0/\sigma$ and $M_0 \equiv m_0/(m + m_0)$. If only the first Sonine correction is retained (which means $a_0 = a = 0$), the solution to Eq. (B1) is

$$D^T[1] = -x_0 \left(\nu_1 - \zeta^{(0)} \right)^{-1} \left[\frac{p m_0}{m^2 n} \left(1 - \frac{\rho T_0}{m_0 p}\right) - \frac{1}{2} \frac{M_0}{m} (1 + \omega)^d \phi \chi_0^{(0)} (1 + \alpha_0) \right]. \quad (\text{B7})$$

Here, $D^T[1]$ denotes the first Sonine approximation to D^T . To close the determination of D^T up to the second Sonine approximation, we multiply now Eq. (23) by $\mathbf{S}_0(\mathbf{V})$ and integrate over velocity to get

$$(\nu_4 - 2\zeta^{(0)})a_0 + \frac{\rho}{n_0 T_0^2} (\nu_5 - \zeta^{(0)})D^T = Z_2, \quad (\text{B8})$$

where

$$Z_2 = -a\nu_6 + \frac{1}{T_0} - \frac{1}{d(d+2)} \frac{m_0}{n_0 T_0^3} \int d\mathbf{v} S_{0,i} \mathcal{K}_{0,i} \left[\frac{\partial}{\partial \mathbf{V}} \cdot (\mathbf{V} f^{(0)}) \right], \quad (\text{B9})$$

$$\nu_4 = -\frac{2}{d(d+2)} \frac{m_0}{n_0 T_0^3} \int d\mathbf{v} \mathbf{S}_0 \cdot J_0^{(0)} [f_{0,M} \mathbf{S}_0, f^{(0)}], \quad (\text{B10})$$

$$\nu_5 = -\frac{2}{d(d+2)} \frac{m_0}{n_0 T_0^2} \int d\mathbf{v} \mathbf{S}_0 \cdot J_0^{(0)} [f_{0,M} \mathbf{V}, f^{(0)}], \quad (\text{B11})$$

$$\nu_6 = -\frac{2}{d(d+2)} \frac{m_0}{n_0 T_0^3} \int d\mathbf{v} \mathbf{S}_0 \cdot J_0^{(0)} [f_0^{(0)}, f_M \mathbf{S}_0]. \quad (\text{B12})$$

The collision integral of (B9) involving the operator $\mathcal{K}_{0,i}$ is given by [15]

$$\begin{aligned} \frac{1}{d} \int d\mathbf{v} \quad S_{0,i}(\mathbf{V}) \mathcal{K}_{0,i} \left[\frac{\partial}{\partial \mathbf{V}} \cdot (\mathbf{V} f^{(0)}) \right] &= -\frac{1}{2} x_0 \frac{n M_0 T^2}{m} (1 + \omega)^d \chi_0^{(0)} \phi (1 + \alpha_0) \left\{ \frac{M\gamma}{M_0} [(d+2)(M_0^2 - 1) \right. \\ &\quad \left. + (2d - 5 - 9\alpha_0)M_0 M + (d - 1 + 3\alpha_0 + 6\alpha_0^2)M^2] + 6M^2(1 + \alpha_0)^2 \right\}, \end{aligned} \quad (\text{B13})$$

where $\gamma \equiv T_0/T$ is the temperature ratio and $M \equiv m/m_0 + m$. In reduced units and by using matrix notation, Eqs. (B1) and (B8) can be rewritten as

$$\begin{pmatrix} \nu_1^* - \zeta^* & \gamma^2 \nu_2^* \\ \frac{\nu_5^* - \zeta^*}{\gamma^2} & \nu_4^* - 2\zeta^* \end{pmatrix} \begin{pmatrix} D^{T*} \\ a_0^* \end{pmatrix} = \begin{pmatrix} X_1^* - \gamma^2 a^* \nu_3^* \\ X_2^* - a^* \nu_6^* \end{pmatrix}. \quad (\text{B14})$$

Here, $\nu_i^* = \nu_i/\nu$, $D^{T*} = (m\nu/x_0T)D^T$, $a_0^* = T^2\nu a_0$, $a^* = T^2\nu a$, and

$$X_1^* = -\left(\frac{m_0p}{mnT} - \gamma\right) + \frac{1}{2}(1+\omega)^d M_0 \chi_0^{(0)} \phi(1+\alpha_0), \quad (\text{B15})$$

$$\begin{aligned} X_2^* &= \gamma^{-1} + \frac{1}{2(d+2)} \frac{M_0^2}{M} (1+\omega)^d \gamma^{-3} \chi_0^{(0)} \phi(1+\alpha_0) \\ &\times \left\{ \frac{M\gamma}{M_0} [(d+2)(M_0^2 - 1) + (2d-5-9\alpha_0)M_0M \right. \\ &\quad \left. + (d-1+3\alpha_0+6\alpha_0^2)M^2] + 6M^2(1+\alpha_0)^2 \right\}. \end{aligned} \quad (\text{B16})$$

The solution to Eq. (B14) provides the explicit expression of the second Sonine approximation $D^T[2]$ to D^T . It can be written in the form (44), where the dimensionless function H is

$$H = \frac{\nu_1^* - \zeta^*}{X_1^*} \frac{(\nu_4^* - 2\zeta^*)(X_1^* - \gamma^2\nu_3^*a^*) - \gamma^2\nu_2^*(X_2^* - \nu_6^*a^*)}{\nu_2^*(\zeta^* - \nu_5^*) + (\nu_1^* - \zeta^*)(\nu_4^* - 2\zeta^*)}. \quad (\text{B17})$$

The determination of the first and second Sonine approximations to the diffusion coefficients D_0 and D follows similar mathematical steps as those made before for D^T . Here, only the final results will be provided. The kinetic diffusion coefficient D_0 is obtained from the integral equation (24) by substitution of the Sonine approximation (35). In matrix notation, the coefficients D_0 and b_0 obey the equation

$$\begin{pmatrix} \nu_1^* - \frac{1}{2}\zeta^* & \gamma^2\nu_2^* \\ \frac{\nu_5^* - \zeta^*}{\gamma^2} & \nu_4^* - \frac{3}{2}\zeta^* \end{pmatrix} \begin{pmatrix} D_0^* \\ b_0^* \end{pmatrix} = \begin{pmatrix} \gamma \\ 0 \end{pmatrix}, \quad (\text{B18})$$

where $D_0^* = (m_0^2\nu/\rho T)D_0$ and $b_0^* = T\nu b_0$. The solution to (B18) gives the second Sonine approximation to D_0 . It can be written as Eq. (42) where the dimensionless function F is

$$F = \left[1 + \frac{\nu_2^*(\zeta^* - \nu_5^*)}{(\nu_1^* - \frac{1}{2}\zeta^*)(\nu_4^* - \frac{3}{2}\zeta^*)} \right]^{-1}. \quad (\text{B19})$$

The corresponding matrix equation defining the coefficients D and c_0 is

$$\begin{pmatrix} \nu_1^* - \frac{1}{2}\zeta^* & \gamma^2\nu_2^* \\ \frac{\nu_5^* - \zeta^*}{\gamma^2} & \nu_4^* - \frac{3}{2}\zeta^* \end{pmatrix} \begin{pmatrix} D^* \\ c_0^* \end{pmatrix} = \begin{pmatrix} Y_1^* - \gamma^2\nu_3^*c^* \\ Y_2^* - \nu_6^*c^* \end{pmatrix}, \quad (\text{B20})$$

where $D^* = (m_0\nu/n_0T)D$, and $c_0^* = nT\nu c_0$. Moreover, the inhomogeneous terms are given by

$$Y_1^* = \zeta^* D^{T*} \left(1 + \phi \frac{\partial \ln \chi^{(0)}}{\partial \phi} \right) - \frac{m_0}{mT} \frac{\partial p}{\partial n} + \frac{1}{2} M_0 \phi (1 + \alpha_0) \left(\frac{1 + \theta}{\theta} \right) \frac{\partial}{\partial \phi} \left(\frac{\mu_0}{T} \right)_{T, n_0}, \quad (\text{B21})$$

$$\begin{aligned} Y_2^* &= \zeta^* a_0^* \left(1 + \phi \frac{\partial \ln \chi^{(0)}}{\partial \phi} \right) + \frac{1}{2(d+2)} \frac{M^2}{M_0} \phi (1 + \alpha_0) \frac{\partial}{\partial \phi} \left(\frac{\mu_0}{T} \right)_{T, n_0} \\ &\times \left\{ [(d+8)M_0^2 + (7+2d-9\alpha_0)M_0M + (2+d+3\alpha_0^2-3\alpha_0)M^2] \theta \right. \\ &\quad \left. + 3M^2(1+\alpha_0)^2\theta^3 + [(d+2)M_0^2 + (2d-5-9\alpha_0)M_0M + (d-1+3\alpha_0+6\alpha_0^2)M^2] \theta^2 \right. \\ &\quad \left. - (d+2)\theta(1+\theta) \right\}, \end{aligned} \quad (\text{B22})$$

where $c^* = nT\nu c$, $\theta = m_0T/mT_0$ is the mean-square velocity of the gas particles relative to that of the intruder particle and

$$a_0^* = \frac{\gamma^{-2}(\zeta^* - \nu_5^*)(X_1^* - \gamma^2\nu_3^*a^*) + (\nu_1^* - \zeta^*)(X_2^* - \nu_6^*a^*)}{\nu_2^*(\zeta^* - \nu_5^*) + (\nu_1^* - \zeta^*)(\nu_4^* - 2\zeta^*)}. \quad (\text{B23})$$

The second Sonine approximation $D[2]$ can be easily obtained from Eq. (B20) and the result can be written in the form (43) where G is

$$G = \frac{\nu_1^* - \frac{3}{2}\zeta^* - \gamma^2\nu_2^*(Y_2^* - \nu_6^*c^*)(Y_1^* - \gamma^2\nu_3^*c^*)^{-1}}{\nu_1^* - \frac{3}{2}\zeta^* + \nu_2^*(\zeta^* - \nu_5^*)(\nu_1^* - \frac{1}{2}\zeta^*)^{-1}}. \quad (\text{B24})$$

Finally, in order to get the explicit dependence of the transport coefficients on dissipation, one still needs to compute the temperature ratio $\gamma = T_0/T$. It is determined from the condition $\zeta_0^* = \zeta^*$, where ζ_0^* is [15]

$$\zeta_0^* = \frac{4\pi^{(d-1)/2}}{d\Gamma(\frac{d}{2})} \left(\frac{\bar{\sigma}}{\sigma}\right)^{d-1} \chi_0^{(0)} M \left(\frac{1+\theta}{\theta}\right)^{1/2} (1+\alpha_0) \left[1 - \frac{M}{2}(1+\theta)(1+\alpha_0)\right]. \quad (\text{B25})$$

APPENDIX C: COLLISION INTEGRALS

In this Appendix we obtain the expressions for the collision frequencies ν_i^* . Except ν_2^* and ν_3^* , the other quantities were already determined [15] for arbitrary composition. For the sake of completeness, we display now their explicit forms in the tracer limit ($x_1 \rightarrow 0$). They are given by

$$\nu_1^* = \frac{2\pi^{(d-1)/2}}{d\Gamma(\frac{d}{2})} \left(\frac{\bar{\sigma}}{\sigma}\right)^{d-1} \chi_0^{(0)} M(1+\alpha_0) \left(\frac{1+\theta}{\theta}\right)^{1/2}, \quad (\text{C1})$$

$$\nu_4^* = \frac{\pi^{(d-1)/2}}{d(d+2)\Gamma(\frac{d}{2})} \left(\frac{\bar{\sigma}}{\sigma}\right)^{d-1} \chi_0^{(0)} M(1+\alpha_0) \left(\frac{\theta}{1+\theta}\right)^{3/2} \left[A - (d+2)\frac{1+\theta}{\theta}B\right], \quad (\text{C2})$$

$$\nu_5^* = \frac{2\pi^{(d-1)/2}}{d(d+2)\Gamma(\frac{d}{2})} \left(\frac{\bar{\sigma}}{\sigma}\right)^{d-1} \chi_0^{(0)} M(1+\alpha_0) \left(\frac{\theta}{1+\theta}\right)^{1/2} B, \quad (\text{C3})$$

$$\nu_6^* = -\frac{\pi^{(d-1)/2}}{d(d+2)\Gamma(\frac{d}{2})} \left(\frac{\bar{\sigma}}{\sigma}\right)^{d-1} \chi_0^{(0)} \frac{M^2}{M_0} (1+\alpha_0) \left(\frac{\theta}{1+\theta}\right)^{3/2} \left[C + (d+2)\frac{1+\theta}{\theta}D\right], \quad (\text{C4})$$

where

$$\begin{aligned} A = & 2M^2 \left(\frac{1+\theta}{\theta}\right)^2 \left(2\alpha_0^2 - \frac{d+3}{2}\alpha_0 + d+1\right) [d+5 + (d+2)\theta] \\ & - M(1+\theta) \{ \lambda\theta^{-2}[(d+5) + (d+2)\theta][(11+d)\alpha_0 - 5d-7] \\ & - \theta^{-1}[20 + d(15-7\alpha_0) + d^2(1-\alpha_0) - 28\alpha_0] - (d+2)^2(1-\alpha_0) \} \\ & + 3(d+3)\lambda^2\theta^{-2}[d+5 + (d+2)\theta] + 2\lambda\theta^{-1}[24 + 11d + d^2 + (d+2)^2\theta] \\ & + (d+2)\theta^{-1}[d+3 + (d+8)\theta] - (d+2)(1+\theta)\theta^{-2}[d+3 + (d+2)\theta], \end{aligned} \quad (\text{C5})$$

$$\begin{aligned} B = & (d+2)(1+2\lambda) + M(1+\theta) \{ (d+2)(1-\alpha_0) - [(11+d)\alpha_0 - 5d-7]\lambda\theta^{-1} \} \\ & + 3(d+3)\lambda^2\theta^{-1} + 2M^2 \left(2\alpha_0^2 - \frac{d+3}{2}\alpha_0 + d+1\right) \theta^{-1}(1+\theta)^2 \\ & - (d+2)\theta^{-1}(1+\theta), \end{aligned} \quad (\text{C6})$$

$$\begin{aligned} C = & 2M^2(1+\theta)^2 \left(2\alpha_0^2 - \frac{d+3}{2}\alpha_0 + d+1\right) [d+2 + (d+5)\theta] \\ & - M(1+\theta) \{ \lambda[d+2 + (d+5)\theta][(11+d)\alpha_0 - 5d-7] \\ & + \theta[20 + d(15-7\alpha_0) + d^2(1-\alpha_0) - 28\alpha_0] + (d+2)^2(1-\alpha_0) \} \\ & + 3(d+3)\lambda^2[d+2 + (d+5)\theta] - 2\lambda[(d+2)^2 + (24 + 11d + d^2)\theta] \\ & + (d+2)\theta[d+8 + (d+3)\theta] - (d+2)(1+\theta)[d+2 + (d+3)\theta], \end{aligned} \quad (\text{C7})$$

$$\begin{aligned}
D = & (d+2)(2\lambda - \theta) + M(1+\theta) \{ (d+2)(1-\alpha_0) + [(11+d)\alpha_0 - 5d - 7]\lambda \} \\
& - 3(d+3)\lambda^2 - 2M^2 \left(2\alpha_0^2 - \frac{d+3}{2}\alpha_{12} + d+1 \right) (1+\theta)^2 + (d+2)(1+\theta), \tag{C8}
\end{aligned}$$

Here, $\lambda = M_0(1-\gamma^{-1})$. It must be noticed that Eqs. (C1)–(C8) have been obtained by taking Maxwellian distributions for the reference homogeneous cooling state distributions $f^{(0)}$ and $f_0^{(0)}$.

It only remains to evaluate the collision integrals defining the collision frequencies ν_2^* and ν_3^* . To compute them, we use the property

$$\begin{aligned}
\int d\mathbf{v}_1 h(\mathbf{v}_1) J_0^{(0)}[\mathbf{V}_1|F, G] = & \chi_0^{(0)} \bar{\sigma}^{d-1} \int d\mathbf{v}_1 \int d\mathbf{v}_2 F(\mathbf{v}_1) G(\mathbf{v}_2) \\
& \times \int d\hat{\boldsymbol{\sigma}} \Theta(\hat{\boldsymbol{\sigma}} \cdot \mathbf{g})(\hat{\boldsymbol{\sigma}} \cdot \mathbf{g}) [h(\mathbf{V}'_1) - h(\mathbf{V}_1)], \tag{C9}
\end{aligned}$$

with

$$\mathbf{V}'_1 = \mathbf{V}_1 - M(1+\alpha_0)(\hat{\boldsymbol{\sigma}} \cdot \mathbf{g})\hat{\boldsymbol{\sigma}}. \tag{C10}$$

Use of this property in Eq. (B4) gives

$$\nu_2^* = \frac{2\pi^{(d-1)/2}}{d\Gamma\left(\frac{d+3}{2}\right)} \left(\frac{\bar{\sigma}}{\sigma}\right)^{d-1} \chi_0^{(0)} M(1+\alpha_0) \theta^{1+\frac{d}{2}} \int d\mathbf{c}_1 \int d\mathbf{c}_2 \mathbf{x} e^{-\theta c_1^2 - c_2^2} \left(\theta c_1^2 - \frac{d+2}{2}\right) (\mathbf{x} \cdot \mathbf{c}_1), \tag{C11}$$

where $\mathbf{c}_i = \mathbf{v}_i/v_0$, $\mathbf{x} = \mathbf{g}/v_0$, and we have taken the Maxwellian approximation (A8) for $f^{(0)}$. The integrals appearing in (C10) can be evaluated by the change of variables $\{\mathbf{c}_1, \mathbf{c}_2\} \rightarrow \{\mathbf{x}, \mathbf{y}\}$, where $\mathbf{y} = \theta\mathbf{c}_1 + \mathbf{c}_2$, the Jacobian being $(1+\theta)^{-d}$. With this change the integrals can be easily performed and the final result is

$$\nu_2^* = \frac{\pi^{(d-1)/2}}{d\Gamma\left(\frac{d}{2}\right)} \left(\frac{\bar{\sigma}}{\sigma}\right)^{d-1} \chi_0^{(0)} M(1+\alpha_0) [\theta(1+\theta)]^{-1/2}. \tag{C12}$$

Similarly, the reduced collision frequency ν_3^* is given by

$$\nu_3^* = -\frac{\pi^{(d-1)/2}}{d\Gamma\left(\frac{d}{2}\right)} \left(\frac{\bar{\sigma}}{\sigma}\right)^{d-1} \chi_0^{(0)} \frac{M^2}{M_0} (1+\alpha_0) \theta^{3/2} (1+\theta)^{-1/2}. \tag{C13}$$

APPENDIX D: MODIFIED SONINE APPROXIMATION

The expression for the kinetic diffusion coefficient D_0^* derived from a modified version of the first Sonine approximation recently proposed [25, 48] is displayed in this Appendix. This coefficient is given by

$$D_0^* = \frac{\gamma}{\nu_D^* - \frac{1}{2}\zeta^*}. \tag{D1}$$

Here,

$$\zeta^* = \frac{\sqrt{2}\pi^{(d-1)/2}}{d\Gamma(d/2)} \chi^{(0)} (1-\alpha^2) \left(1 + \frac{3}{32}e\right) \tag{D2}$$

where e is the fourth cumulant of the gas distribution function $f^{(0)}$. It measures the departure of $f^{(0)}$ from its Maxwellian form and its expression is [61]

$$e(\alpha) = \frac{32(1-\alpha)(1-2\alpha^2)}{9+24d-(41-d)\alpha+30\alpha^2(1-\alpha)}. \tag{D3}$$

The (reduced) collision frequency ν_D^* is given by [25]

$$\nu_D^* = \frac{2\pi^{(d-1)/2}}{d\Gamma\left(\frac{d}{2}\right)} \left(\frac{\bar{\sigma}}{\sigma}\right)^{d-1} \chi_0^{(0)} M(1+\alpha_0) \left(\frac{1+\theta}{\theta}\right)^{1/2} \left[1 + \frac{1}{16} \frac{(3+4\theta)e_0 - \theta^2 e}{(1+\theta)^2}\right], \tag{D4}$$

where e_0 is the corresponding fourth cumulant for the distribution function $f_0^{(0)}$ of the intruder. Its explicit form can be found in the Appendix of Ref. [62].

-
- [1] J. Ferziger and H. Kaper, *Mathematical Theory of Transport Processes in Gases* (North-Holland, Amsterdam, 1972).
- [2] J. R. Dorfman and H. van Beijeren, The Kinetic Theory of Gases, Berne, B. J. editor, *Statistical Mechanics, Part B* (New York, Plenum, 1977), pages 65–179.
- [3] H. van Beijeren and M. H. Ernst, *Physica* **68**, 437 (1973).
- [4] M. López de Haro, E. G. D. Cohen and J. M. Kincaid, *J. Chem. Phys.* **78**, 2746 (1983).
- [5] J. T. Jenkins and F. Mancini, *Phys. Fluids A* **1**, 2050 (1989).
- [6] P. Zamankhan, *Phys. Rev. E* **52**, 4877 (1995).
- [7] B. Arnarson and J. T. Willits, *Phys. Fluids* **10**, 1324 (1998).
- [8] J. T. Willits and B. Arnarson, *Phys. Fluids* **11**, 3116 (1999).
- [9] V. Garzó and J. W. Dufty, *Phys. Rev. E* **60**, 5706 (1999).
- [10] P. A. Martin and J. Piasecki, *Europhys. Lett.* **46**, 613 (1999).
- [11] A. Santos and J. W. Dufty, *Phys. Rev. Lett.* **97**, 058001 (2006).
- [12] See for instance, J. M. Montanero and V. Garzó, *Gran. Matt.* **4**, 17 (2002); A. Barrat and E. Trizac, *Gran. Matt.* **4**, 57 (2002); S. R. Dahl, C. M. Hrenya, V. Garzó, and J. W. Dufty, *Phys. Rev. E* **66**, 041301 (2002); R. Pagnani, U. M. B. Marconi, and A. Puglisi, *Phys. Rev. E* **66**, 051304 (2002); P. E. Krouskop and J. Talbot, *Phys. Rev. E* **68**, 021304 (2003); H. Wang, G. Jin, and Y. Ma, *Phys. Rev. E* **68**, 031301 (2003); M. Schröter, S. Ulrich, J. Kreft, J. B. Swift, and H. L. Swinney, *Phys. Rev. E* **74**, 011307 (2006).
- [13] R. D. Wildman and D. J. Parker, *Phys. Rev. Lett.* **88**, 064301 (2002); K. Feitosa and N. Menon, *Phys. Rev. Lett.* **88**, 198301 (2002).
- [14] V. Garzó, J. W. Dufty and C. M. Hrenya, *Phys. Rev. E* **76**, 031303 (2007).
- [15] V. Garzó, C. M. Hrenya and J. W. Dufty, *Phys. Rev. E* **76**, 031304 (2007).
- [16] V. Garzó and J. W. Dufty, *Phys. Rev. E* **59**, 5895 (1999).
- [17] J. F. Lutsko, *Phys. Rev. E* **72**, 021306 (2005).
- [18] V. Garzó and J. W. Dufty, *Phys. Fluids* **14**, 1476 (2002).
- [19] V. Garzó and J. M. Montanero, *Phys. Rev. E* **68**, 041302 (2003).
- [20] V. Garzó and J. M. Montanero, *Phys. Rev. E* **69**, 021301 (2004).
- [21] I. Goldhirsch, *Annu. Rev. Fluid Mech.*, **22**, 57 (2003).
- [22] M. Huthmann, J. A. G. Orza and R. Brito, *Gran. Matt.* **2**, 189 (2000).
- [23] N. V. Brilliantov and T. Pöschel, *Europhys. Lett.* **74**, 424 (2006).
- [24] S. H. Noskovicz, O. Bar-Lev, D. Serero and I. Goldhirsch, *Europhys. Lett.* **79**, 60001 (2007).
- [25] V. Garzó, F. Vega Reyes, and J. M. Montanero, *J. Fluid Mech.* **623**, 387 (2009). e-print ArXiv: 0808.1858 [cond-mat.stat-mech].
- [26] M. G. Clerc, P. Cordero, J. Dunstan, K. Huff, N. Mújica, D. Risso and G. Varas, *Nature Phys.* **4**, 249 (2008).
- [27] F. Vega Reyes and J. S. Urbach, *Phys. Rev. E* **78**, 051301 (2008).
- [28] I. Goldhirsch and G. Zanetti, *Phys. Rev. Lett.* **70**, 1619 (1993).
- [29] J. T. Jenkins and D. K. Yoon, *Phys. Rev. Lett.* **88**, 194301 (2002).
- [30] L. Trujillo, M. Alam and H. J. Herrmann, *Europhys. Lett.* **64**, 190 (2003).
- [31] J. J. Brey, M. J. Ruiz-Montero and F. Moreno, *Phys. Rev. Lett.* **95**, 098001 (2005).
- [32] V. Garzó, *Phys. Rev. E* **78**, 020301(R) (2008).
- [33] G. A. Bird, *Molecular Gas Dynamics and the Direct Simulation Monte Carlo of Gas Flows* (Clarendon, Oxford, 1994).
- [34] J. J. Brey, M. J. Ruiz-Montero, D. Cubero, and R. García-Rojo, *Phys. Fluids* **12**, 876 (2000).
- [35] S. Chapman and T. G. Cowling, *The Mathematical Theory of Nonuniform Gases* (Cambridge University Press, Cambridge, 1970).
- [36] A. Goldshtein and M. Shapiro, *J. Fluid Mech.* **282**, 41 (1995).
- [37] J. J. Brey, J. W. Dufty, and A. Santos, *J. Stat. Phys.* **87**, 1051 (1997).
- [38] J. W. Dufty, *Adv. Complex Systems* **4**, 397 (2002).
- [39] E. A. Mason, *J. Chem. Phys.* **22**, 169 (1954).
- [40] M. López de Haro and E. G. D. Cohen, *J. Chem. Phys.* **80**, 408 (1984).
- [41] N.F. Carnahan and K.E. Starling, *J. Chem. Phys.* **51**, 635 (1969).
- [42] T. Boublik, *J. Chem. Phys.* **53**, 471 (1970); E. W. Grundke and D. Henderson, *Mol. Phys.* **24**, 269 (1972); L. L. Lee and D. Levesque, *Mol. Phys.* **26**, 1351 (1973).
- [43] T. M. Reed and K. E. Gubbins, *Applied Statistical Mechanics* (McGraw-Hill, New York, 1973), Chap. 6.
- [44] J. Jenkins and F. Mancini, *J. Appl. Mech.* **54**, 27 (1987).
- [45] A. Santos, private communication.
- [46] J. A. McLennan, *Introduction to Nonequilibrium Statistical Mechanics* (Prentice-Hall, New Jersey, 1989).
- [47] Please notice that using the same number of simulated particles for both species does not imply that their densities are equal: the very small concentration limit for the tracer particles is implied by the form of the two kinetic equations that

are simulated.

- [48] V. Garzó, A. Santos, and J. M. Montanero, *Physica A* **376**, 94 (2007).
- [49] J. J. Brey and M. J. Ruiz-Montero, *Phys. Rev. E* **70**, 051301 (2004); J. J. Brey, M. J. Ruiz-Montero, P. Maynar and I. García de Soria, *J. Phys.: Condens. Matter* **17**, S2502 (2005).
- [50] See for instance, A. Kudrolli, *Rep. Prog. Phys.* **67**, 209 (2004).
- [51] J. Kincaid, E. G. D. Cohen and M. López de Haro, *J. Chem. Phys.* **86**, 963 (1987).
- [52] M. Alam, L. Trujillo and H. J. Herrmann, *J. Stat. Phys.* **124**, 587 (2006).
- [53] A symbolic code that calculates the transport coefficients worked out in this article is at the disposal of the reader in the webpage: [http : //www.unex.es/fisteor/vicente/granular_files.html](http://www.unex.es/fisteor/vicente/granular_files.html).
- [54] V. Garzó, *Europhys. Lett.* **75**, 521 (2006).
- [55] J. F. Lutsko, J. J. Brey, J. W. Dufty, *Phys. Rev. E* **65**, 051304 (2002).
- [56] A. Santos, V. Garzó and J. W. Dufty, *Phys. Rev. E* **69**, 061303 (2004).
- [57] J. J. Brey, M. J. Ruiz-Montero and D. Cubero, *Phys. Rev. E* **60**, 3150 (1999); J. J. Brey, M. J. Ruiz-Montero, F. Moreno and R. García-Rojo, *Phys. Rev. E* **65**, 061302 (2002).
- [58] E. C. Rericha, C. Bizon, M. D. Shattuck and H. L. Swinney, *Phys. Rev. Lett.* **88**, 014302 (2001).
- [59] X. Yang, C. Huan, D. Candela, R. W. Mair and R. L. Walsworth, *Phys. Rev. Lett.* **88**, 044301 (2002); C. Huan, X. Yang, D. Candela, R. W. Mair and R. L. Walsworth, *Phys. Rev. E* **69**, 041302 (2004).
- [60] V. Garzó, J. M. Montanero, and J. W. Dufty, *Phys. Fluids* **18**, 083305 (2006).
- [61] T. P. C. van Noije and M. H. Ernst, *Gran. Matt.* **1**, 57 (1998).
- [62] V. Garzó, *J. Stat. Mech.: Theory Exp.* P05007 (2008).